

Research Highlights

[FY2023]

Japan International Research Center for Agricultural Sciences

**Meeting global challenges through
research and technology development**



Meta-analysis reveals general rice ratooning ability, and rice ratoon cropping shifts the plant type from panicle weight type to panicle number type

Rice ratooning is a cultivation method that omits seedling raising, puddling, and transplanting and is therefore attracting attention as a low-input and low-cost method. However, it faces the challenge of significantly lower yields compared to conventional double-cropped rice. To address this, many studies have been conducted on the identification of varieties and traits with high ratooning ability. However, due to differences in genetic and environmental factors, there are various results from many studies, making it difficult to understand the ratooning ability of rice.

This report uses statistical analysis of 51 field experiment data collected from 14 countries from 1976 to 2022 to examine the general ratooning ability, the effect of genetic and environmental factors on the ratooning ability of yield-related traits (plant height, number of stems, panicle length, number of spikelets, number of panicles, 1000-grain weight, grain-filling rate, growth period, and grain yield), and the relationship between ratooning ability and yield. In this study, ratooning ability is defined as the growth ratio of the ratoon crop to the main crop (ratoon rate).

The growth period of ratoon rice was 41% shorter than that of the main crop, and the number of spikelets and grain yield were significantly reduced by 48% and 56%, respectively, while the number of stems and panicles increased by only 19% (Fig. 1). This suggests that ratoon rice cultivation can accelerate heading, and the plant architecture shifts from the panicle weight type in the main crop to the panicle number type in the ratoon crop (Fig. 2). The influence of the number of stems in ratoon rice on ratoon rate was more variable and more susceptible to the effects of genetic and environmental factors such as variety and cultivation environment, while the number of spikelets, growth period, and 1000-grain weight were relatively less affected (Fig. 3). Path analysis between ratoon rates of each yield-related trait shows that growth period had a significant direct effect on grain yield, plant height, and panicle length, and that panicle length had a significant direct effect on the number of spikelets (Fig. 4). In other words, the results suggest that the shortening of the growth period of ratoon rice accelerates heading, which restricts the growth of the stem apex and the differentiation of young panicles that determine the number of spikelets, while the number of panicles does not increase significantly, resulting in a decrease in grain yield.

Authors: Shiraki, S. [JIRCAS],
Kywae, Thura, Lae, L.M., Thin, M.C., Kyaw, M., Nwe, N., May, T.O., Loon, P.P., Aung, K.T. [DAR]

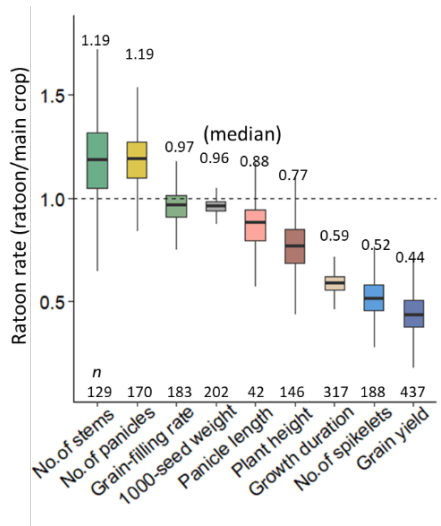


Fig. 1. Ratoon rate (final amount of growth in the ratoon crop relative to that in the main crop) for each yield-related trait

Boxplots show the distribution of the data. *n* indicates the number of data shown in the figure.

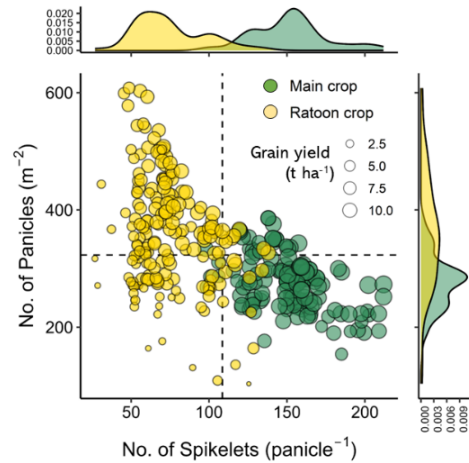


Fig. 2. Relationship between number of panicles and number of spikelets for main and ratoon crops

The number of data *n* = 170.

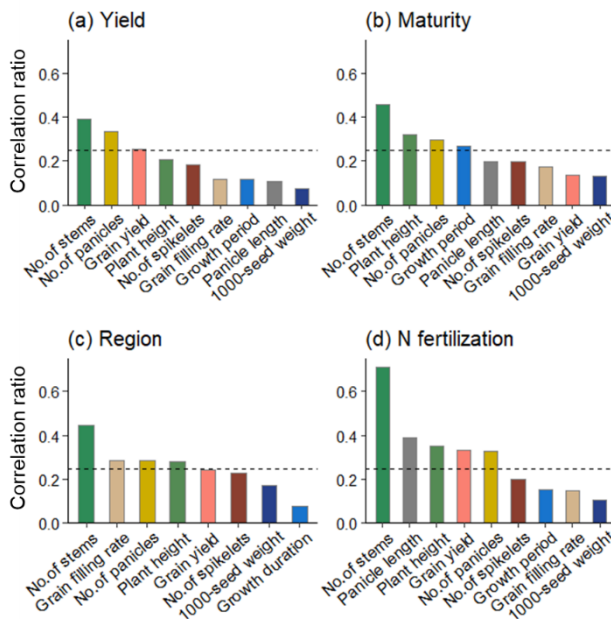


Fig. 3. Effects of differences in genetic and environmental factors such as variety and cultivation condition on the ratoon rate of yield-related traits

Correlation ratio indicates the ratio of the weighed variance of the group means divided by the variance of all samples on ratoon rate. The groups are divided into (a) yield: low (4.0 t ha⁻¹), medium (6.5 t ha⁻¹), high (9.0 t ha⁻¹), (b) maturity: early (110 days), medium (130 days), late (147 days), (c) region: South and Southeast Asia, East Asia, America, Africa, and (d) N fertilization: low (< 100 kg N ha⁻¹), medium (300 kg N ha⁻¹ > N ≥ 100 kg N ha⁻¹), and high (≥ 300 kg N ha⁻¹).

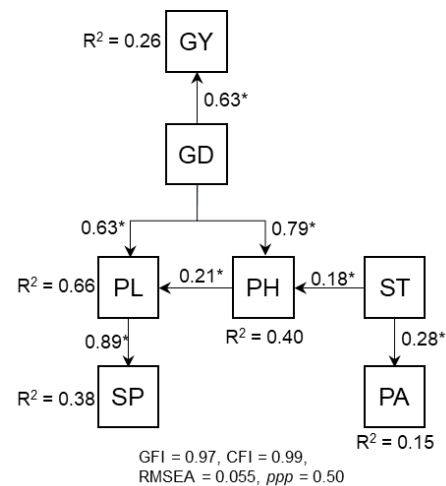


Fig. 4. Path analysis of the influence of features associated with yield on the ratoon rate

GY, grain yield; PH, plant height; ST, stem number; PA, panicle number; SP, spikelet number; PL, panicle length; GD, growth duration; sample size, *n* = 42; *, statistically significant pathways; GFI, goodness of fit index; CFI, comparison fit index; RMSEA, root mean square error of approximation; *ppp*, posterior predictive *p*-value.

High-efficiency microbial saccharification with novel xylan-saccharifying bacteria

Lignocellulosic biomass is attracting attention as the world's most abundant renewable resource, and its effective utilization is being sought. However, the development of an efficient and cost-effective technology for biomass saccharification is a challenge, and JIRCAS has developed the "microbial saccharification method," which does not rely on commercial cellulose saccharification enzymes (cellulases), but only on the cultivation of saccharifying microorganisms (see FY2022 Research Highlights: Technology development to saccharify cellulose "only by cultivating microorganisms" without using cellulase enzymes).

Some agricultural waste biomass contains not only cellulose but also a large amount of xylan. Since xylan inhibits the saccharification of cellulase enzyme, it is necessary to search for xylan-saccharifying microorganisms that can be incorporated into microbial saccharification methods and to develop saccharification technology using such microorganisms. We screened microorganisms that efficiently saccharify xylan at 60°C under anaerobic conditions using xylan as the sole carbon source and obtained DA-C8 bacteria. The characteristics of the DA-C8 bacteria isolated in this study are reported.

We have screened microorganisms that efficiently saccharify xylan from Ishigaki Island compost at 60°C under anaerobic conditions using a medium containing xylan as the sole carbon source and obtained DA-C8 bacteria. This bacterium belongs to the same phylogenetic lineage as the known *Xylanibacillus composti*, but based on genetic, chemotaxonomic, and phylogenetic analyses (including digital DNA-DNA hybridization), average amino acid sequence identity values, and major polar lipid composition, a new genus and species, *Insulambacter* and *I. thermoxylanivorax*, were proposed (Fig. 1). *I. thermoxylanivorax* DA-C8 not only can completely saccharify xylan (Fig. 2) but also hemicelluloses other than xylan, such as arabinoxylan and galactan. It also grows over a wide temperature (37–60°C; optimum temperature: 55°C) and pH range (4–11; optimum pH: 9). In a microbial saccharification test using oil palm fiber (EFB), which contains relatively high amounts of xylan, the saccharification capacity of *Clostridium thermocellum* alone was 24.7% and 13.2% for *I. thermoxylanivorax* DA-C8, which has a high cellulose saccharification capacity. When *I. thermoxylanivorax* DA-C8 and *C. thermocellum* were co-cultured, the saccharification efficiency was 58.1%, showing an extremely high saccharification efficiency. This is a 2- to 4-fold increase in saccharification efficiency compared to each alone (Fig. 3). *I. thermoxylanivorax* DA-C8 has been deposited as a reference strain at the RIKEN BioResource Center (JCM 34211T) and the German Microbial Cell Culture Collection Center (DSM 111723T) and is available for distribution.

Authors: Kosugi, A., Uke, A. [JIRCAS]

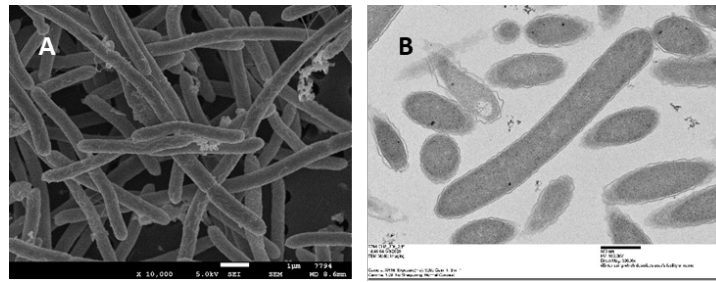


Fig. 1. Cell morphology of *I. thermoxylanivorax* strain DA-C8 cultured in xylose carbon source medium

A. Scanning electron microscopy image of *I. thermoxylanivorax* DA-C8. White scale bar is 1 µm;
B. Transmission electron microscopy image of a thin section of *I. thermoxylanivorax* DA-C8 strain.

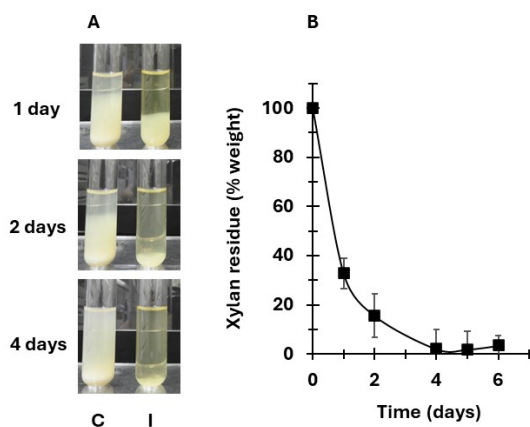


Fig. 2. Xylan saccharification capacity of *I. thermoxylanivorax* DA-C8

A. Xylan saccharification by *I. thermoxylanivorax* DA-C8 in 1% xylan carbon source medium. Days 1, 2, and 4 after inoculation with *I. thermoxylanivorax* DA-C8. C: uninoculated, I: inoculated with *I. thermoxylanivorax* DA-C8;
B. Residual percentage of xylan over time in 1% xylan carbon source medium.

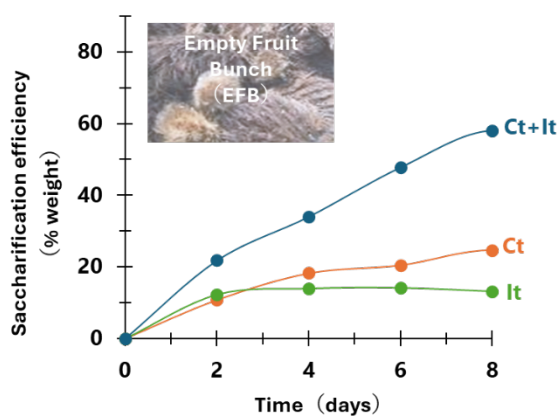


Fig. 3. Microbial saccharification by co-culture of *I. thermoxylanivorax* DA-C8 and *C. thermocellum*

Microbial saccharification was measured in a medium containing 1% EFB fiber. Comparison of saccharification capacity of *C. thermocellum* alone (Ct), *I. thermoxylanivorax* DA-C8 alone (It), and *C. thermocellum* in co-culture with *I. thermoxylanivorax* DA-C8 (Ct+It), which has high cellulose saccharification capacity used in the microbial saccharification method.

References: 1) Chhe et al. (2021) Characterization of a thermophilic facultatively anaerobic bacterium *Paenibacillus* sp. strain DA-C8 that exhibits xylan degradation under anaerobic conditions. *J. Biotechnol.* 342: 64–71.

<https://doi.org/10.1016/j.jbiotec.2021.10.008> © Elsevier B.V. 2021

2) Chhe et al. (2023) *Int J Syst Evol Microbiol.* 73(3): 005724. © The Author(s) 2023

The figures were reprinted/modified from Chhe et al. (2021) with permission.

Waterlogging due to rainfall alters gene expression patterns in the upper stem of oil palm

Palm oil accounts for approximately 36% of global vegetable oil production, making it the most abundant. However, the majority of this production occurs in Southeast Asia, specifically in Indonesia and Malaysia. The geographical concentration of production systems is considered vulnerable to climate change. To reveal the weather factors affecting oil palm (*Elaeis guineensis*), we comprehensively analyzed the gene expression levels of oil palm tissues collected over time (transcriptome analysis). By examining the relationship between meteorological factors and oil palm, we can unravel its physiological responses to environmental conditions. Understanding oil palm's physiological responses to environmental factors can help identify vulnerabilities to climate change and contribute to sustainable oil palm plantation management.

At the research site in Lampung Province, Indonesia, samples were collected from the leaf and stem tissues of oil palm for transcriptome analysis over a time series (Figs. 1 and 2). Sampling was conducted approximately nine times over two years (T1 to T9). Notably, during sampling at T3 and T7, there were rainfall events exceeding 80 mm per day. The gene expression profiles of samples obtained from the oil palm stem tissues at T3 and T7 differed significantly from those at other time points (Fig. 3). However, there was no clear relationship between the gene expression profiles from both tissues and the daily average temperature or cumulative temperature. To investigate the gene expression patterns related to waterlogging, we categorized genes into those associated with waterlogging and those unrelated, based on homology searches with the model plant *Arabidopsis thaliana*. In the trunk tissues, the proportion of genes related to waterlogging showed significant expression variation in both upregulation and downregulation compared to other gene groups. Conversely, such a trend was not observed in leaf tissues (Fig. 4). The homology search results for *A. thaliana* and oil palm revealed substantial differences in gene expression levels related to low oxygen response and oxygen levels. Additionally, changes in gene expression related to ethylene response were evident, indicating stress responses to waterlogging (Fig. 5). These findings suggest that while mature oil palms exhibit resilience to temperature fluctuations, they are sensitive to stress responses in stem tissues under short-duration, heavy rainfall conditions, highlighting their vulnerability to waterlogging.

Authors: Tani, N., Arai, T., Kondo, T., Kosugi, A. [JIRCAS],
Irawati, D., Nugroho, S. [UGM], Lim, H. [Univ. of Tsukuba]

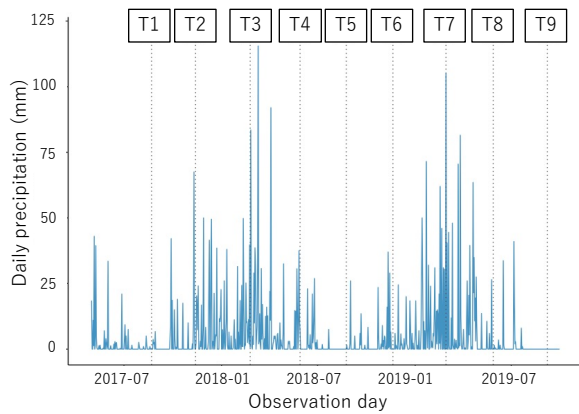


Fig. 1. Daily precipitation at the study site (Lampung Province, Indonesia) during the observation period

T1 to T9 indicate sampling dates for transcriptome analysis.

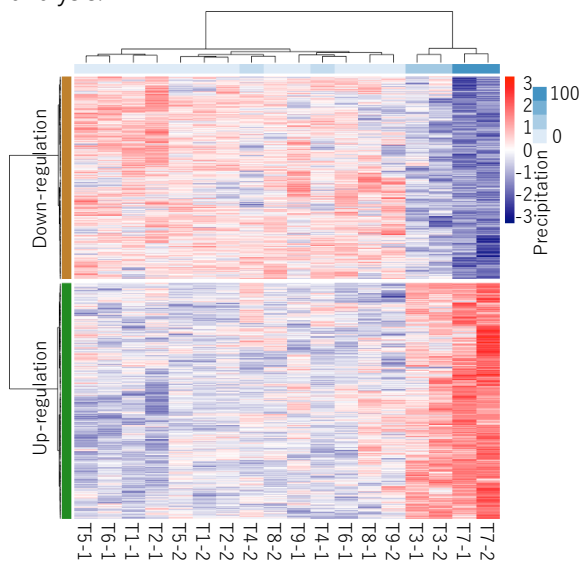


Fig. 4. Proportion of differentially expressed genes in waterlogging-related gene sets and other gene sets during waterlogging

Distinct patterns of gene expression, especially in stem between waterlogging-related genes and other gene sets, were found when investigating the proportion of differentially expressed genes (diagonal in the bars) during waterlogging (T3 and T7).

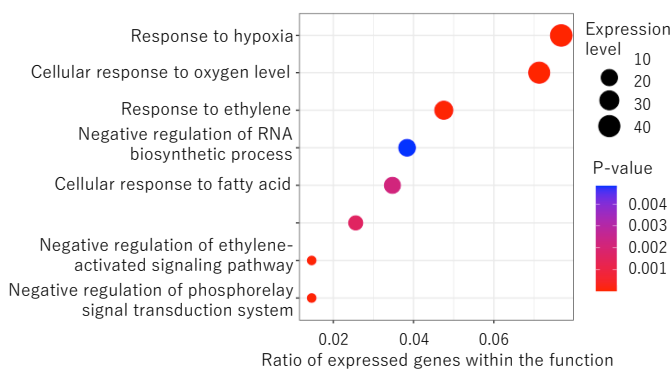


Fig. 2. Studying and sampling of old palm trunk tissue

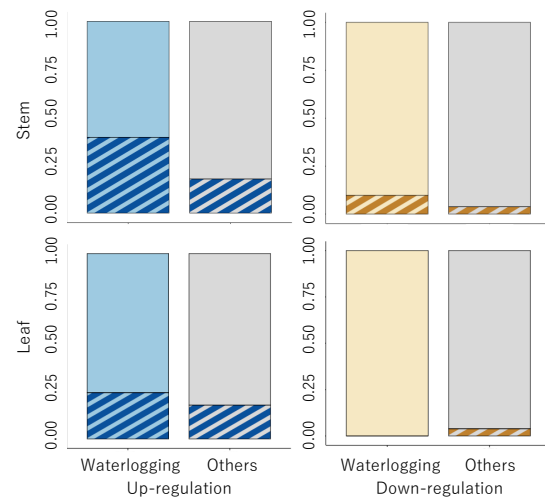


Fig. 3. Heatmap of the gene expression profile of stem

By arranging profiles based on daily precipitation, a heatmap reveals significant differences in gene expression profiles between T3, T7, and other samples with high daily precipitation.

Fig. 5. Functions of genes differentially expressed during waterlogging in stems

We found that significantly differentially expressed genes are primarily associated with low-oxygen response and oxygen levels. Additionally, changes in gene expression related to ethylene response were also observed.

Reference: Lim et al. (2023) *Frontiers in Plant Science* 14: 1213496. © The Author(s) 2023
The figures were modified from Lim et al. (2023)

Identification of the key biological nitrification inhibition (BNI) compound from maize roots

Specific plants can suppress nitrification in soil by releasing inhibitory natural products from their roots, a chemical-ecological phenomenon called biological nitrification inhibition (BNI). BNI utilization is a useful strategy for solving environmental problems (e.g., water pollution by NO_3^- ; production of the greenhouse gas N_2O) and improving nitrogen uptake while reducing nitrogen losses from agricultural fields. The crucial property for the isolation of BNI compounds is whether their root exudates, extracts, and compounds are water-insoluble (hydrophobic) or water-soluble (hydrophilic). While hydrophobic compounds with lower mobility are retained in the rhizosphere, hydrophilic compounds can move further away from the roots. In a previous study, two major hydrophobic BNI-contributing compounds from the root surface (zeanone and HDMBOA) were identified in maize, together with two analogs of HDMBOA from inside the roots (Fig. 1). Our objective in this study is to identify the chemical structure and function of a hydrophilic BNI-active compound from maize.

The most BNI-active compound in hydrophilic BNI-activity from maize roots was identified as 6-methoxy-2(3*H*)-benzoxazolone (MBOA). MBOA has been detected in several *Poaceae* species such as maize and wheat. MBOA strongly inhibited the growth of *Nitrosomonas europaea* (Fig. 2). In a soil incubation experiment, NO_3^- production was suppressed in the presence of MBOA during incubation for 4 days, and BNI-activity declined in parallel with MBOA biodegradation after incubation for 5 days (Fig. 3). Further experiments suggested that two benzoxazinoids, HDMBOA and HDMBOA- β -glucoside, which are chemically and biologically unstable in soil, respectively, could be converted into the more stable BNI-active MBOA in the soil (Fig. 4). Therefore, MBOA is a key component in the BNI-activity of maize.

MBOA is degraded in soil via microbial reaction, while new MBOA can be constantly produced and released by living maize. Hence, maize can stably exhibit BNI activity. The BNI compounds identified in our study are a promising indicator for evaluating BNI capacity among maize species, and can lead to the development of BNI-enhanced maize.

Authors: Otaka, J., Yoshihashi, T., Subbarao, G.V., MingLi J., [JIRCAS],
Ono, H., [NARO]

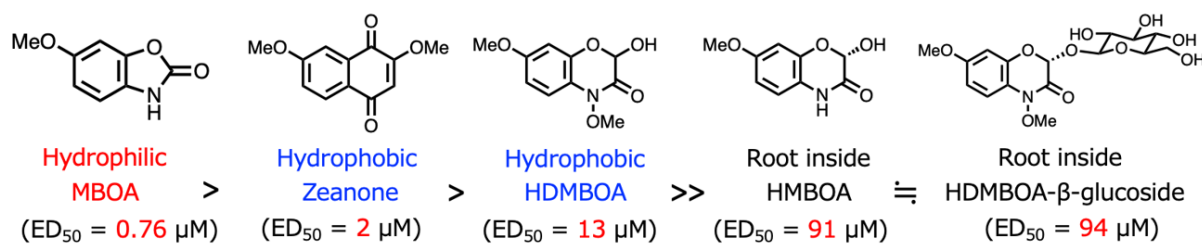


Fig. 1. Structures and BNI activities of identified BNI compounds from maize roots
 The values in the parentheses indicate BNI activities. A smaller value means stronger BNI activity.

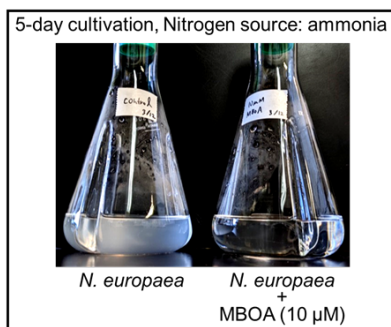


Fig. 2. Effect of MBOA on the growth of *N. europaea*
 (Left) *N. europaea* in cloudy medium; (Right) Clear medium caused by suppression of the growth of *N. europaea* in the presence of MBOA.

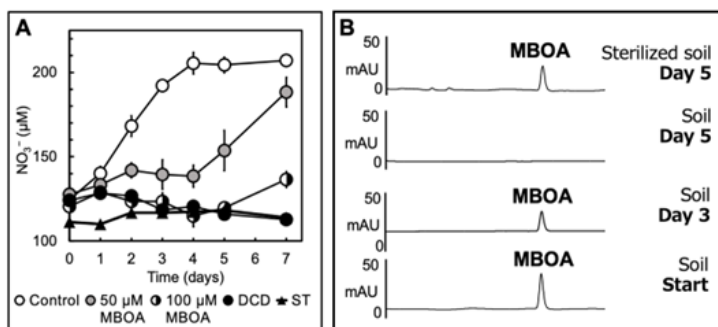


Fig. 3. Effect of MBOA on nitrification and its stability in soil incubation test

Soil was incubated under the presence of MBOA, and the concentrations of NO_3^- and MBOA were time-dependently measured. Day 0 (start) means the result 1 hour after application of MBOA. (A) Control: water was used instead of MBOA., DCD: chemical nitrification inhibitor dicyandiamide, ST: sterilized soil. (B) Concentration of MBOA was measured by HPLC.

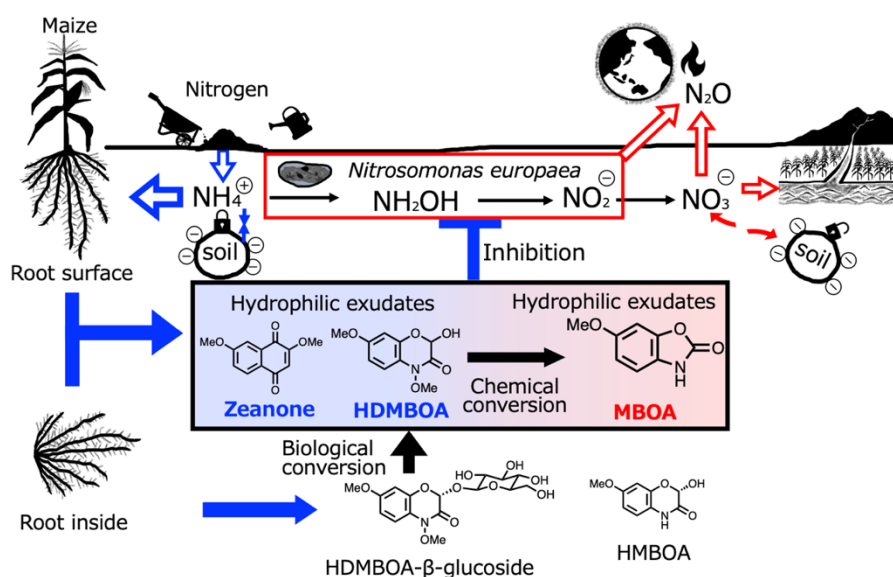


Fig. 4. BNI mechanism of maize

BNI of maize is exhibited by three BNI-active compounds including the key MBOA.

Reference: Otaka, et al. (2023) *Plant Soil* 489: 341-359. © The Author(s) 2023
 The figures were reprinted/modified from Otaka et al. (2023)

Development of models to predict stem diameter and tree height of *Shorea platyclados* (Dipterocarpaceae) based on genomic information from seedlings

In recent years, rapid advancements in DNA sequencing technology have made it relatively inexpensive to collect genomic information even for woody plants that are close to wild species. However, for woody plants with large individual sizes and long lifespans, evaluating the performance of next generations (known as progeny trial) after breeding superior individuals requires vast land and time for their growth. This becomes a limiting factor in selecting superior individuals. Therefore, attention is now focused on methods that utilize genomic information to predict specific phenotypes. Specifically, if we can predict future phenotypes using genomic information from offspring, it becomes possible to overcome previous limiting factors. In this study, we aimed to develop a genomic selection model for *Shorea macrophylla*, a tree species in the Dipterocarpaceae, which is expected to be intensively planted in Southeast Asian tropical forests.

We established a workflow using a training population of a progeny trial forest with relatively less environmental heterogeneity for genomic selection (GS) model. We collected genomic information and focal phenotypes. Using these data, we corrected the spatial structure of the phenotypes due to environmental heterogeneity, detected important genetic markers by genome-wide association study (GWAS), and established a workflow for developing GS models (Fig. 1). The workflow was implemented using scripts in R and Python, which we have made publicly available. By selecting highly correlated markers based on GWAS results, we achieved usable predictive accuracy using both linear models (6 algorithms) and nonlinear models (6 algorithms). With this model, it becomes possible to select offspring based on genomic information from the training population without the subsequent progeny testing (Table 1). This approach promises to enhance breeding outcomes related to growth. Specifically, when predicting the 7-year diameter growth, we calculated the median of predictive accuracy for 100 randomly generated models using linear and nonlinear methods. Given that diameter growth results from a combination of primary and secondary growth, the use of nonlinear models, which can account for interactions among numerous genes, yielded higher predictive accuracy (Fig. 2). Conversely, tree height, being only influenced by primary growth, was associated with fewer relevant genes. Therefore, narrowing down the number of associated genes through GWAS led to a more accurate GS model. (Fig. 3)

Authors: Tani, N. [JIRCAS],
Na'iem, M., Widiyatno, Indrioko, S., Sawitri [UGM], Akutsu, H., Tsumura, Y. [Univ. of Tsukuba]

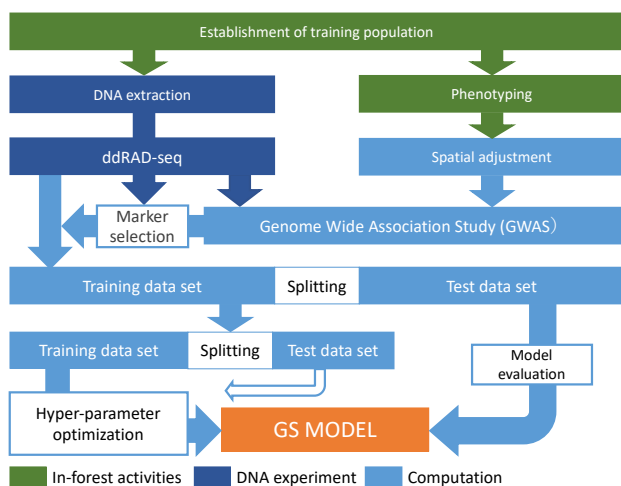


Fig. 1. Workflow for GS model

This script, which includes the calculation process highlighted in light blue, has been publicly released.

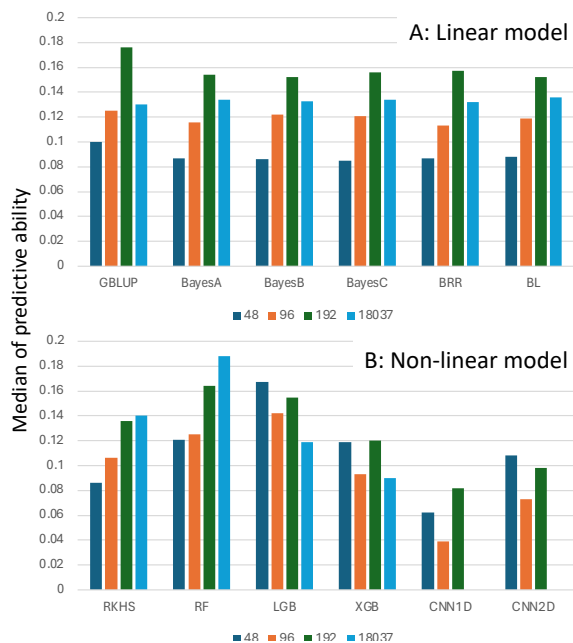


Fig. 2. Median of predictive accuracy of GS models for diameter growth in the 7th year of planting

By GWAS, 48, 96, and 192 DNA markers were selected from a total of 18037 DNA markers, Median was calculated from the 100 replicates for linear algorithms in A and non-linear algorithms in B. Due to the computational burden, CNN1D and CNN2d do not use all markers.

Table 1. The maximum predictive ability for diameter growth and tree height

Trait	Number of markers	Maximum predictive ability	Algorithm
D7	48	0.279	BRR
	96	0.342	CNN1D
	192	0.291	CNN1D
	18037	0.440	XGB
H7	48	0.343	XGB
	96	0.427	BayesB
	192	0.354	LGB
	18037	0.297	LGB

D7 and H7 represent diameter growth and tree height in the seventh year of planting, respectively. The maximum predictive accuracy was obtained from 10 trials of 10 training data (total of 100 trials) and using the algorithm when the 48, 96, and 192 markers were selected by GWAS from a total of 18037 markers.

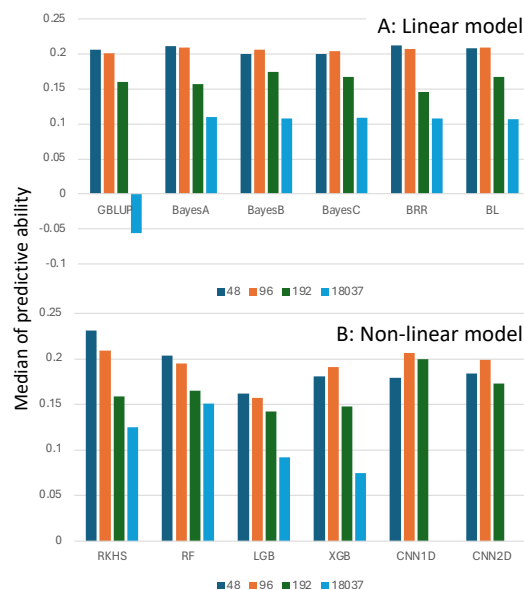


Fig. 3. Median of predictive accuracy of GS models for tree height in the 7th year of planting

See footnote in Fig. 2.

Reference: Akutsu et al. (2023) *Frontiers in Plant Science* 14: 1241908. © The Author(s) 2023
The figures were modified from Akutsu et al. (2023)

Drought resilience of interspecific hybrids of the tropical forest trees *Shorea leprosula* and *S. curtisii*

Climate change is predicted to increase drought frequency and intensity in the tropical rainforest regions of Southeast Asia, and there is concern that trees with low drought tolerance will die or grow poorly. The dipterocarp family, which dominates the forests of this region, is important as a timber resource. Among them, *Shorea leprosula* (Fig. 1) is suitable as plantation species due to its fast growth rate, but has the disadvantage of low drought tolerance. *S. curtisii*, on the other hand, grows slowly and takes longer to harvest, but can also be grown on dry ridges. An interspecific hybrid can combine the various characteristics of both parents and be used to create superior crop varieties. However, the characteristics of hybrids in dipterocarp trees are unknown. In this study, we investigated the leaf and branch characteristics associated with drought tolerance in interspecific hybrid seedlings between *S. leprosula* and *S. curtisii* to explore the potential for using hybrids to create varieties with high resilience to climate change.

First, we compared leaf morphology and physiological characteristics. *S. leprosula* had the thinnest leaves but also had the highest proportion of palisade layer with a higher photosynthetic capacity. On the other hand, *S. curtisii* had a thick cuticle and epidermis that protected the leaves from desiccation, but the proportion of the palisade layer was low. Hybrids had leaves with medium characteristics or almost the same as in the parent species (Fig. 2). The photosynthetic capacity of *S. leprosula* was higher than that of *S. curtisii*, consistent with its faster growth rate. The capacity of the hybrid was intermediate between the parental species and is likely to grow faster than *S. curtisii* (Table 1). Second, we compared the pattern in which branches lose their water-permeating function under drought stress, and *S. curtisii* and hybrids were found to be more drought-tolerant than *S. leprosula* (Fig. 3). Finally, we artificially dried the soil and examined changes in leaf drought tolerance. The lower leaf osmotic potential in hybrids and *S. curtisii* indicated that they had a greater ability for osmotic regulation under drought conditions than *S. leprosula*. When drought tolerance was assessed by leaf wilting point (water potential at loss of turgor pressure), the leaves of *S. leprosula* wilted easily, but the hybrids and *S. curtisii* did not wilt easily and had high drought tolerance (Table 1).

Overall, it was clear that the leaves and branches of the hybrid are more drought-tolerant than *S. leprosula*. This suggests that hybrids can be used to create varieties with high drought resilience, helping tropical forestry adapt to climate change.

Authors: Tanaka, K. [JIRCAS],
Ichie, T., Norichika, Y. [Kochi Univ.], Kamiya, K. [Ehime Univ.],
Inoue, Y. [FFPRI], Ngo, K. M., Lum, S. K. Y. [Nanyang Tech. Univ.]

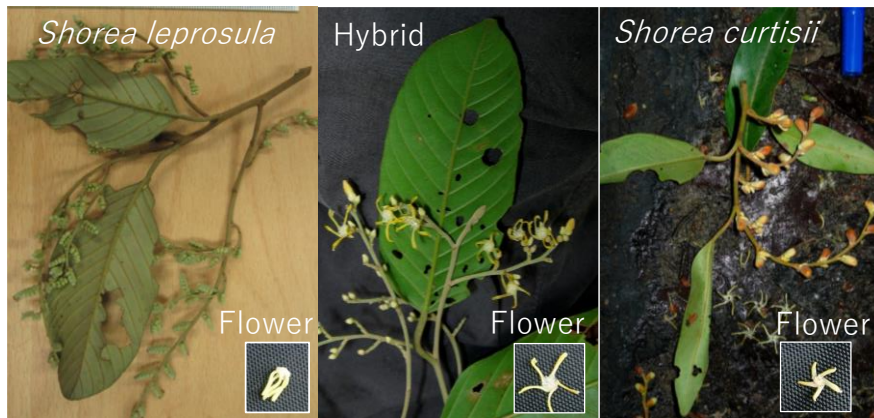


Fig. 1. Flowers and leaves of *S. leprosula* and *S. curtisii* and their hybrid
 The petals of *S. leprosula* are closed and twisted, but those of *S. curtisii* are open. Hybrid flowers are open, but the petals are twisted, inheriting the characteristics of both parents.

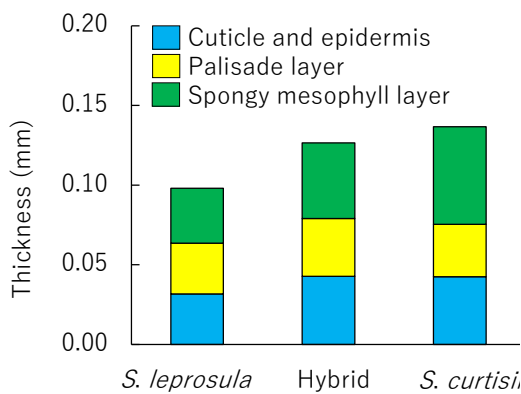


Fig. 2. Thickness of leaf internal tissue
 Leaf surfaces with thick epidermis and cuticle significantly suppress water loss, making them more drought-tolerant, whereas those with thick palisade layers contribute to photosynthesis.

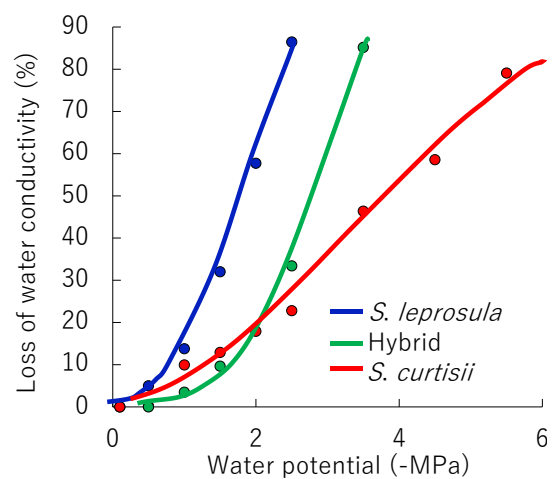


Fig. 3. Branch water conductivity under drought stress
 A greater water potential means higher drought stress, which inhibits water flow in the branch. *S. leprosula* easily lost water conductivity under mild drought stress.

Table 1. Leaf photosynthetic rate, osmotic potential, and turgor loss point under drought stress

	Photosynthetic rate ($\mu\text{mol m}^{-2} \text{s}^{-1}$)	Osmotic potential (MPa)	Turgor loss point (MPa)
<i>S. leprosula</i>	3.16a	-1.18a	-1.33a
Hybrid	2.44ab	-1.40b	-1.53b
<i>S. curtisii</i>	2.09b	-1.54b	-1.72c

Lower turgor loss point means that the leaves are more resistant to wilting and more drought-tolerant. Different alphabets indicate statistically significant differences.

Reference: Kenzo et al. (2023) *Forest Ecology and Management* 548: 121388. © Elsevier B.V. 2023
 Figures and table reprinted/modified from Kenzo et al. (2023) with permission.

The difference in biochar application depths affects nitrate leaching and water budget

The Haber–Bosch process enables humanity to produce nitrogen fertilizer, allowing the population to grow by increasing food production. However, the global nitrogen cycle is disturbed beyond the planetary boundary. Nitrogen applied as fertilizer often leaches from farmland in nitrate form, moving into the groundwater, rivers, and other water bodies and polluting the surrounding environment. Therefore, mitigating nitrogen leaching is urgently required. Biochar has been applied to farmlands to mitigate leaching while storing carbon. The effect of biochar application differs depending on the application depth; however, the effect of the application depth remains unclear. This study aimed to evaluate the effects of the biochar application depth on nitrogen leaching and soil water conditions.

We conducted a pipe experiment with no plant using bagasse biochar (800 °C) with four treatments: no biochar application (control), surface application (0 – 5 cm), plow layer application (0 – 30 cm), and subsurface application (25 – 30 cm). The experiment was conducted in a glass room. The amount of applied biochar was the same among the treatments (10 t ha⁻¹). Biochar content rates (expressed as weight ratios) in the biochar amendment layer were 1.57% for surface/subsurface application and 0.26% for plow layer application. Surface irrigation was conducted every two or three days, and powdered fertilizer was applied monthly. We measured the amount of drainage and nitrate leaching during the experiment. The results showed that the drainage and nitrate leaching amounts differed depending on biochar application depths. Nitrate leaching tended to be reduced by surface application, whereas drainage and leaching were reduced by plow layer application. Subsurface application did not alter drainage and leaching. We estimated the water budget for each treatment. Compared with the control, soil evaporation tended to reduce under surface application, whereas it tended to increase under plow layer application.

Our study indicated that, although the same amount of biochar was applied, the effect of biochar application differs depending on the application depth. Surface and plow layer applications reduced nitrate leaching; the change in soil moisture conditions might induce these differences. Choosing a proper biochar application depth could contribute to mitigating nitrate leaching and possibly reducing nitrogen fertilizer use.

Authors: Hamada, K., Nakamura, S., Kanda, T. [JIRCAS]

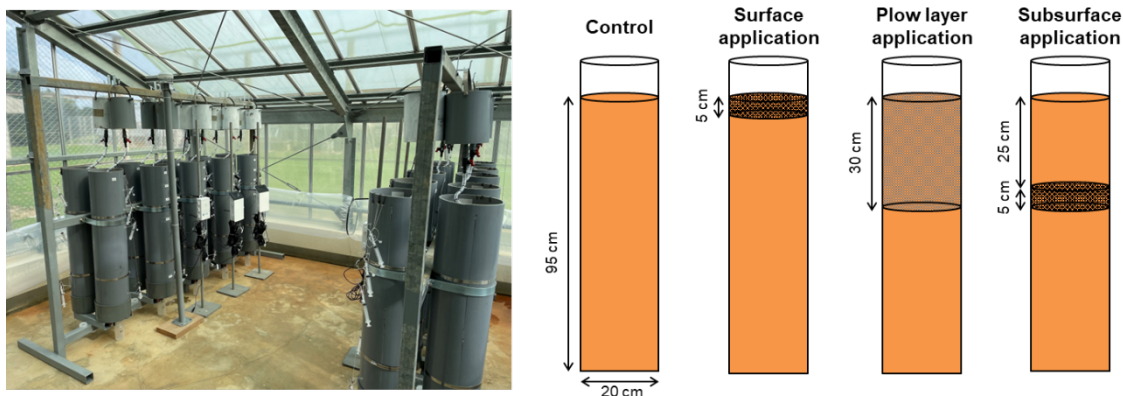


Fig. 1. Pipe experiment

The pipe experiment was conducted from August to November in a glass room. We applied four treatments with five replicates. The soil bulk density was set to 1.25 g cm⁻³.

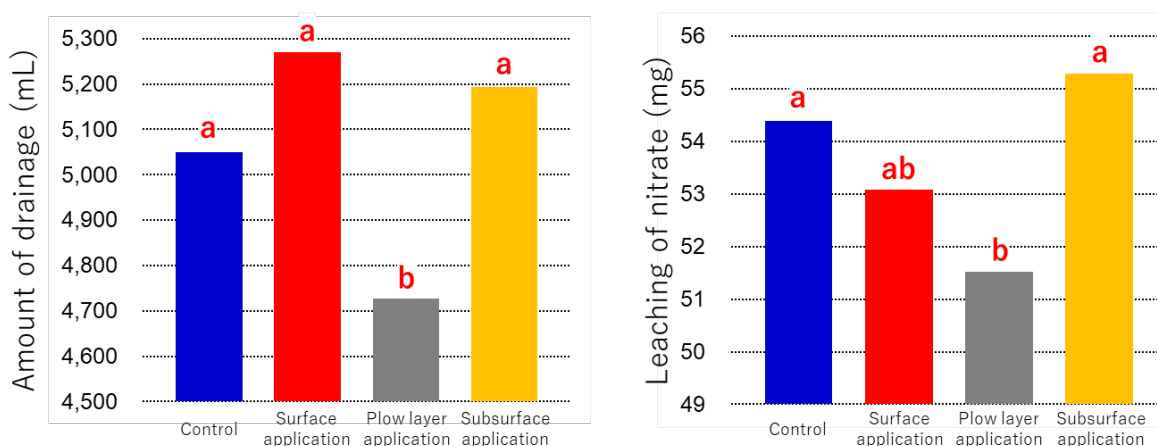


Fig. 2. Cumulative amount of drainage (left) and nitrate (right)

Letters indicate significant difference ($p < 0.005$).

Table 1. Water budget within the pipes

	Control	Surface application	Plow layer application	Subsurface application
Irrigation (mL)			14,850	
Evaporation (mL)	8,960	8,754	9,389	9,149
Water in the pipe (mL)	6,977	7,175	6,860	6,964
Drainage (mL)	5,049 ^a	5,269 ^a	4,726 ^b	5,194 ^a

Water in the pipe was calculated by multiplying sensor values ($n=2$) at depths of 10, 20, 35, and 80 cm by soil layer volumes. Evaporation was calculated using the amount of irrigation, drainage, and water in the pipe. Letters show significant difference ($p < 0.05$).

Reference: Hamada K, Nakamura S, Kanda T, Takahashi M. (2023) Effects of biochar application depth on nitrate leaching and soil water conditions. *Environmental Technology*. <https://doi.org/10.1080/09593330.2023.2283403>.

© 2023 Informa UK Limited, trading as Taylor & Francis Group

Figures and table reprinted/modified from Hamada et al. (2023) with permission.

Unraveling the factors influencing spatiotemporal variations in riverine dissolved organic matter and iron through a machine learning approach

Dissolved organic matter (DOM) serves vital functions in aquatic ecosystems, such as regulating light availability in the water column and providing energy and nutrients to microorganisms, while excessive loading of light-absorbing colored DOM reduces light penetration, inhibiting photosynthesis by primary producers (e.g., phytoplankton, seaweeds). DOM also serves as an organic ligand for iron, an essential micronutrient for primary producers, and increases its availability. Based on the result of periodic water quality monitoring in the rivers of Ishigaki Island, a tropical island of Japan, the factors influencing spatiotemporal variations in the concentrations of riverine DOM and its components were identified by analyzing their relationships with catchment properties (e.g., land use, soil type) and seasonality (e.g., water temperature). Furthermore, the impact of the molecular composition of DOM on the concentration of dissolved iron (DFe) was assessed. The random forest (RF) machine learning algorithm was employed for the analyses because of its flexibility in handling non-parametric datasets and non-linear relationships, and its ability to measure the importance of predictor variables.

The RF models using catchment properties and water temperature as predictor variables accurately predicted the concentration of dissolved organic carbon (DOC) and the abundance of three humic-like components (C1 ~ C3) identified by fluorescence excitation-emission matrix coupled with parallel factor analysis (EEM-PARAFAC). Water temperature and areal share of poorly-drained lowland soil (Gleyic Fluvisols) were identified as the most important predictor variables for DOC and the humic-like components (Table 1) and positively influenced these DOM parameters (Fig. 1). This result indicates that the concentrations of DOC and humic-like components exhibit clear seasonal variations with their maxima in summer and that the poorly-drained lowland soil serves as the major source of riverine DOM (particularly humic-like components) in the studied catchments. The RF model for DFe using the abundance of EEM-PARAFAC components and other parameters relevant to iron solubility (e.g., water temperature, pH, concentrations of Ca^{2+} and Mg^{2+}) as predictor variables also explained a large portion of the variation in DFe concentration. A humic-like component derived from terrestrial material (C1) was the most important predictor variable and had a positive relation to DFe concentration (Fig. 2), emphasizing its significance as an organic ligand for iron.

The results obtained in this study improve our understanding of the spatiotemporal variability of terrestrial DOM and iron loadings and their impacts on tropical coastal ecosystems of high ecological and economic importance.

Authors: Kikuchi, T., Anzai, T. [JIRCAS]

Table 1. Importance of the predictor variables in the random forest (RF) models for dissolved organic carbon (DOC) and three humic-like components (C1 ~ C3)

Variable	DOC	C1	C2	C3
Water temperature	16.1	20.8	21.3	17.5
Land use				
Upland fields	10.8	9.1	11.2	10.0
Pastures	11.2	8.8	11.5	9.9
Paddy fields	9.7	7.5	9.3	8.1
Forests	14.1	11.1	13.2	11.9
Livestock barns	7.0	8.0	7.2	8.2
Soil				
Haplic Acrisols (Chromic)	11.9	11.1	11.3	10.9
Haplic Cambisols	12.3	9.9	12.4	10.2
Haplic Acrisols	12.7	8.9	8.3	8.6
Haplic Cambisols (Eutric)	8.1	7.0	6.3	6.1
Haplic Regosols (Calcaric)	7.7	6.7	6.2	5.8
Gleyic Fluvisols	16.1	22.2	16.8	21.4
Population density	11.7	9.6	8.9	8.6

C1: Derived from terrestrial material by photochemical degradation
 C2: Produced during microbial degradation of organic matter
 C3: Produced during breakdown of lignin (e.g., syringaldehyde)

(%)
 ~25
 ~20
 ~15
 ~10

Importance was measured as the increase in mean squared error (MSE; in %) that occurred when the fitted model was run with the randomly permuted variable of interest. The greater the value, the more important the variable. Values greater than 15% are shown in white bold letters.

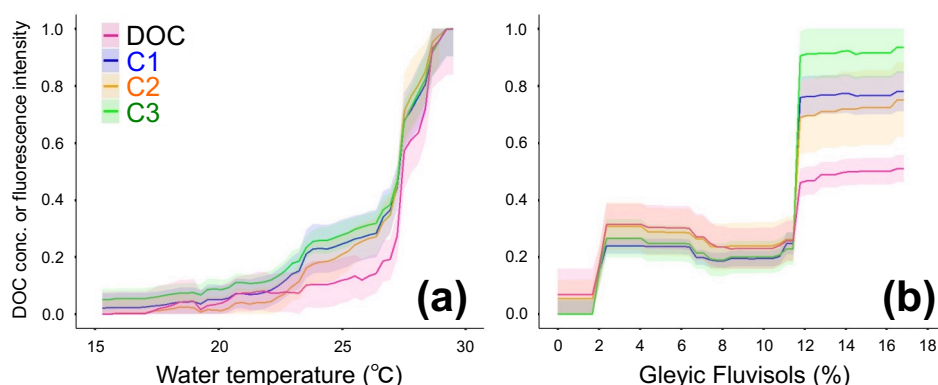


Fig. 1. Partial dependence plots (PDPs) of DOC and humic-like components on (a) water temperature and (b) areal share of Gleyic Fluvisols in the catchment

Solid lines and shaded areas represent the mean partial dependence and its standard deviation, respectively, for 15 RF models generated through three repetitions of five-fold cross-validation. The y-axes are scaled to a difference between the maximum and minimum values of each DOM parameter that is common in both panels.

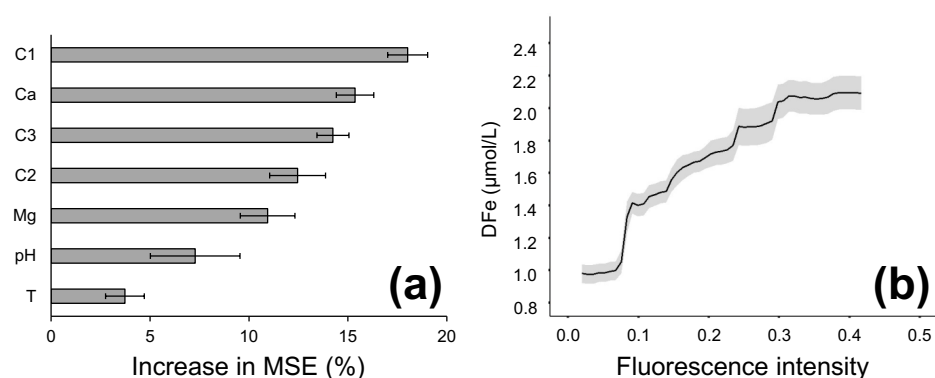


Fig. 2. (a) Importance of the predictor variables in the RF models for dissolved iron (DFe) and (b) PDP of DFe on a humic-like component (C1)

The bars and error bars in 'panel a' represent the mean value and standard deviation, respectively, for 15 RF models from three repetitions of five-fold cross-validation. T denotes water temperature.

Reference: Kikuchi, T., Anzai, T., Ouchi, T. (2023) Assessing spatiotemporal variability in the concentration and composition of dissolved organic matter and its impact on iron solubility in tropical freshwater systems through a machine learning approach. *Science of the Total Environment* 904: 166892. © Elsevier B.V.

Table and figures reprinted/modified from Kikuchi et al. (2023) with permission.

Visualizing the mitigation effect of nitrogen load and chemical fertilizer use, and resource recycling using the food nitrogen footprint concept

The recent price hikes in fertilizers, feeds, and food threaten the global food system, people's livelihoods, and food security. This unstable global situation seriously affects small islands because they heavily rely on importing food and chemical fertilizers to sustain food supply and production. Chemical fertilizer is essential for crop production. However, inefficient use of fertilizers causes considerable loss of reactive nitrogen (Nr) to the environment through volatilization, leaching, and run-off. This phenomenon pollutes the atmosphere, groundwater, and surface water bodies, damaging the environment. To reduce the release of Nr into the environment, we should minimize the use of chemical fertilizers and promote the efficient reuse of regional resources, such as livestock manure. Farmers alone cannot improve nitrogen flow in the food system. The cooperation of consumers, the main driving force of nitrogen flow in the food system, is also essential. The nitrogen footprint is a simple quantitative indicator of the reality and problems of the nitrogen cycle and is useful for sharing results among stakeholders, including consumers. In this study, we aimed to evaluate the present nitrogen flow in the food system of Ishigaki Island, located in the subtropical zone of Japan, and propose a measure to improve it based on the nitrogen footprint concept.

We calculated Nr loss under the present condition of Ishigaki Island using statistical data. It aimed to assess the nitrogen load of the island's entire food system, including imported food and feed and exported food. The study also explored scenarios for achieving a 30% reduction in chemical fertilizer use, a goal of the Sustainable Food Systems Strategy, MIDORI, by maximizing the use of livestock manure on farmland. The results showed that by utilizing 70% of cattle manure on farmland, Nr inputs to crop production could be maintained even with a 30% reduction in chemical fertilizer use, ultimately reducing total Nr loss on Ishigaki Island by 18%.

The food nitrogen footprint applied in this study holds promise for similar tropical and subtropical island regions. It aligns with the United Nations Sustainable Development Goals (SDGs) and the Sustainable Food Systems Strategy, MIDORI. It is expected to aid in the development of strategies to address the recent volatility in chemical fertilizer prices.

Authors: Hamada, K., Oka, N.. [JIRCAS],
Eguchi, S., Hirano, N., Asada, K. [NARO]

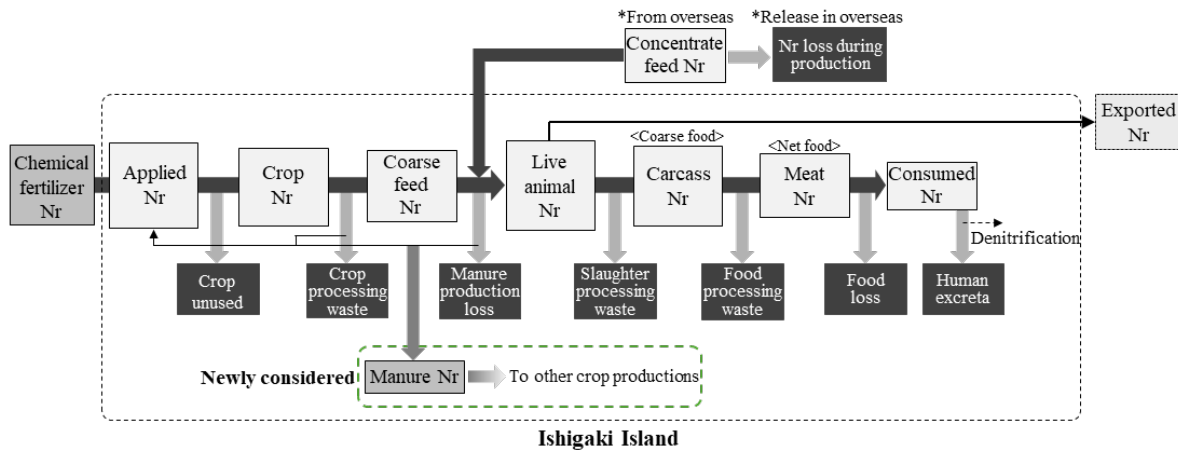
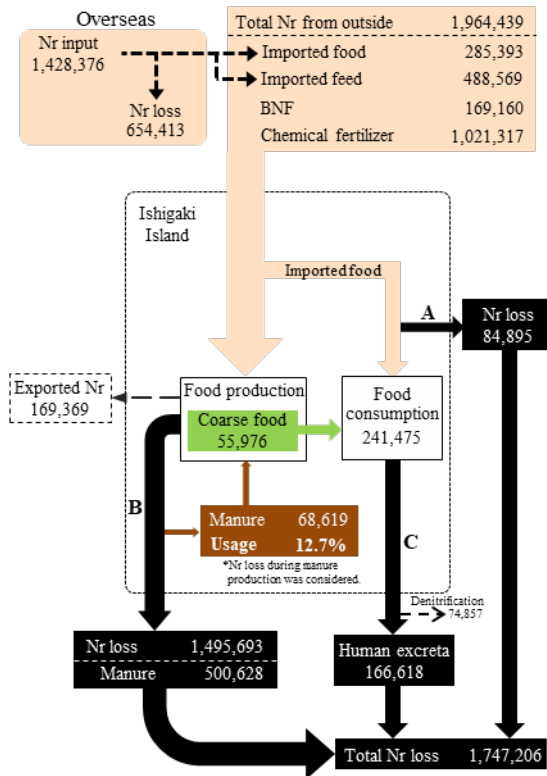


Fig. 1. Schematic for calculating nitrogen flow in livestock production

Nr represents reactive nitrogen. The present study newly considered manure distribution to other crop production.

(a) Nitrogen flow under present condition (kgN)



(b) Nitrogen flow under scenario condition (kgN)

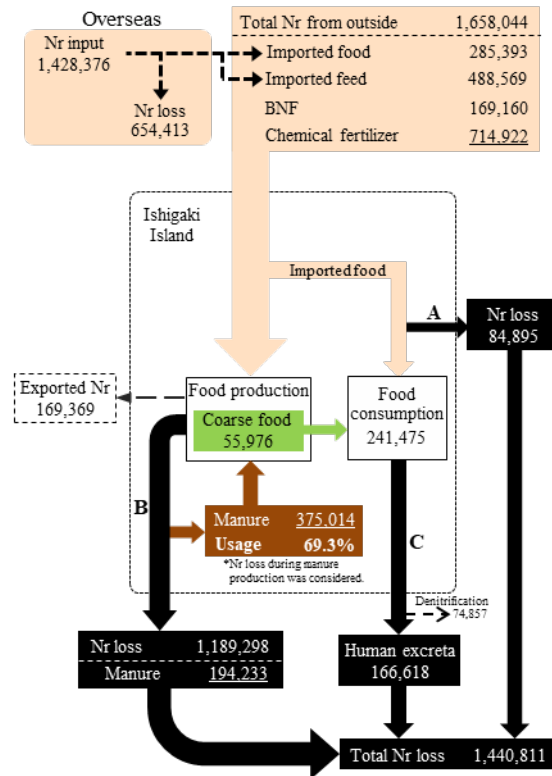


Fig. 2. Nitrogen flow under the (a) present and (b) scenario conditions

Nr is reactive nitrogen, BNF is biological nitrogen fixation, and 'denitrification' is the removed Nr by denitrification from human excreta during sewage treatment. The underlined values indicate differences between the present and scenario conditions. Arrows A–C represent food processing waste and food loss of imported coarse food (A), all Nr losses excluding human excreta in the food system (B), and human excreta after food consumption (C).

Reference: Hamada et al. (2023) *Environmental Research Letters* 18: 075010. © The Author(s) 2023
The figures were reprinted/modified from Hamada et al. (2023).

A QTL allele from wild soybean enhances protein content without reducing the oil content

Soybean, which contains approximately 40% protein and 20% oil, is one of the most important sources of protein and oil for human consumption, providing over 71% of the world's plant-based protein and more than 29% of the oil. Generally, soybean protein content shows a negative correlation with oil content, making it difficult to develop varieties with high protein and oil content. Therefore, it is necessary to identify new genes involved in soybean protein and oil content. Wild soybean, the ancestor of cultivated soybean, possesses higher seed protein content than cultivated varieties. Therefore, wild soybean is a valuable genetic resource that could enhance the protein content of cultivated varieties.

To identify the genes responsible for increasing protein content in wild soybean, a population comprising 113 BC₄F₆ chromosome segment substitution lines (CSSL) was developed from a cross between soybean cultivar 'Jackson' and wild soybean accession JWS156-1. The CSSL population was cultivated in field conditions for 3 years (2018, 2019, and 2020), and the seeds harvested from each line were analyzed for protein and oil contents using the Infratec NOVA instrument. Additionally, quantitative trait locus (QTL) analysis was performed using 243 SSR markers. As a result, we identified 12 QTLs on eight chromosomes associated with seed protein, oil, and protein + oil contents. Among them, the wild soybean allele of protein QTL *qPro19* located on chromosome 19 was confirmed to increase protein content without reducing oil content in soybean seeds. To validate the effect of *qPro19*, near-isogenic lines (NILs) for *qPro19* were developed. Analysis of protein and oil contents showed that the wild soybean type NIL exhibited higher protein content compared to the cultivated soybean type NIL, but there was no significant difference in oil content. Furthermore, BC₄ line T-678, which introduced the *qPro19* allele of wild soybean into another soybean variety, 'Tachiyutaka,' showed enhanced seed protein content without reducing the seed oil content.

The wild soybean allele of the protein content QTL *qPro19* identified in this study can be utilized as genetic material for developing soybean varieties with high levels of both protein and oil content, as well as for improving protein content in specific soybean varieties.

Authors: Park, C., Xu, D. [JIRCAS]

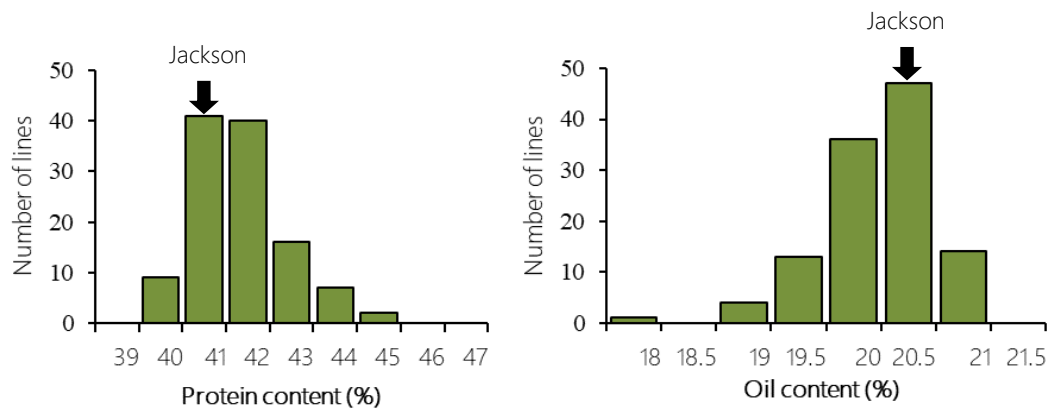


Fig. 1. Frequency distribution of seed protein content (L) and oil content (R) in the wild soybean CSSL population

The protein content and oil content represent the average values over three years from 2018 to 2020. Arrows indicate the observed values for 'Jackson.'

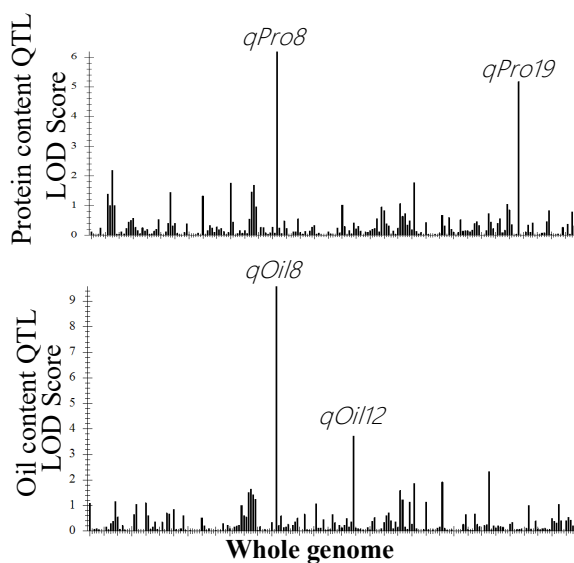


Fig. 2. QTL analysis results of protein content and oil content in the wild soybean CSSL population

QTLs were detected based on the average values over three years. *qPro19* detected on chr 19 is the focus of this study. *qPro8* and *qOil8* detected on chr 8 are previously reported for protein and oil contents. *qOil12* is a minor QTL for oil content. LOD value: A statistical estimate of whether a trait is linked to a certain locus.

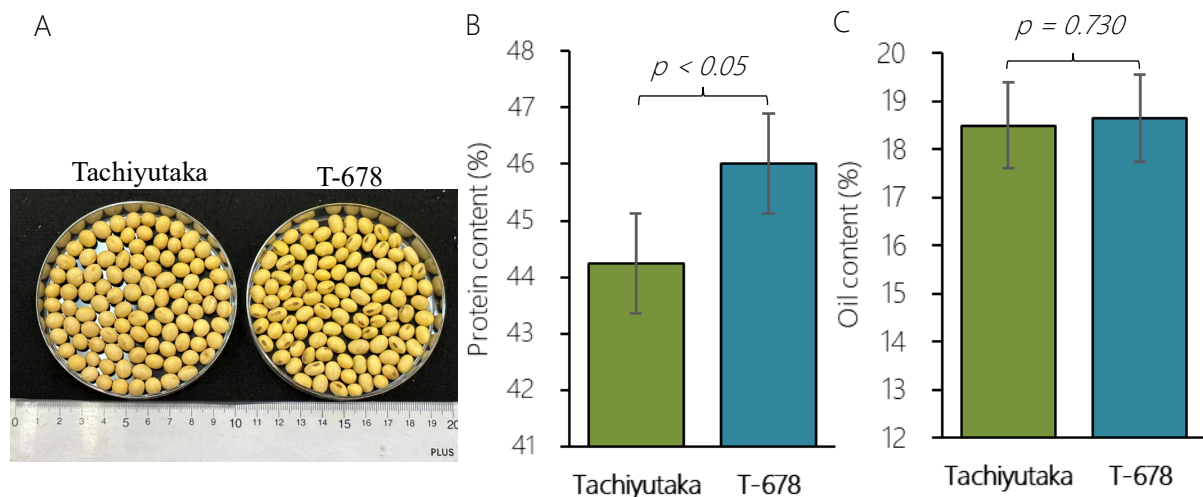


Fig. 3. The allele effect of *qProzz19* in a BC₄F₆ backcrossing line T-678

(A) Appearance of 'Tachiyutaka' and T-678 seeds, (B) Protein content, and (C) Oil content. Error bar means standard deviation.

Reference: Park et al. (2023) *Plant Genetic Resources* 21: 409–417. © The Author(s) 2023.

Figures reprinted/modified from Park et al. (2023)

Development of the drought stress experimental system in the field with ridges

The frequency and damage of droughts have been increasing in recent years, threatening the world's food supply. To develop drought-tolerant crops, many drought studies have been conducted, mainly in the laboratory, and the drought stress response mechanisms of plants have been elucidated at the molecular level. On the other hand, it has been pointed out that the drought stress response of plants in the field differs in some respects from the response mechanisms that have been elucidated in the laboratory, and there are still many unknowns. In the development of drought-tolerant crops, it is essential to conduct drought tolerance tests and elucidate the drought response mechanisms of plants in the field, but it is not easy to reproduce a constant drought environment in the field where the environment fluctuates irregularly.

To overcome the various problems associated with drought trials in the field, we focused on "ridges." During 6 years of trials, we showed that the volumetric water content (VWC) in ridges (ridge height, 30 cm) was consistently lower than that in the flats (Fig. 1A). We also demonstrated that there was no significant difference in the contents of nutrients, nitrogen (N), phosphorus (P), and potassium (K) between the flats and ridges, both at the beginning and at the end of the soybean growing season (Fig.1B). We compared soybean growth in this system. The aboveground biomass of plants grown on ridges was clearly reduced compared with that of plants grown on flats; consequently, the yield of soybean grown on ridges was also reduced compared with that of soybean grown on flats (Fig. 2). The negative effect of ridges on plant growth and yield was complemented by irrigation, indicating that the reduction in plant growth on the ridges was mainly due to lack of water (Fig. 3). Together, these observations demonstrate that ridges are a valuable tool for inducing conditions that mimic mild drought stress in the field.

Although the height and width of the ridges need to be considered depending on the target plants, soil type, and desired level of drought stress, the developed drought stress experimental system is applicable to fields in various regions of the world and is expected to facilitate the selection and production of drought-tolerant lines.

Authors: Nagatoshi, Y., Kobayashi, Y., Fujii, K., Baba, J., Fujita, Y., Ikazaki, K., Oya, T. [JIRCAS]

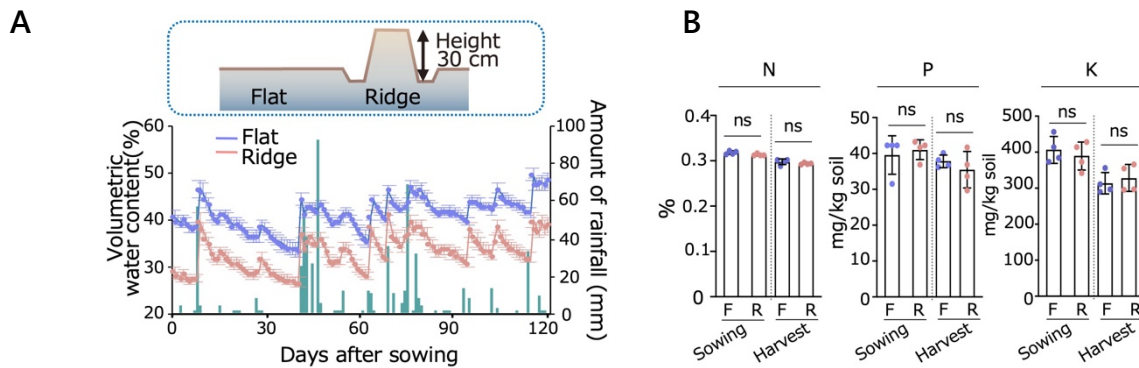


Fig. 1. Soil moisture variability and soil nutrient composition in the field drought stress experimental system with ridges

(A) Time course of soil VWC in the flats (no ridges) and 30-cm high ridges during soybean-growing season. A 30-cm-long soil moisture sensor (TDR) and a temperature sensor were inserted in each test plot, and data were recorded over time by a data logger. $n = 4$, error bars indicate SD. Green bars indicate precipitation. (B) Nutrient contents of soil in flats and ridges at soybean sowing and harvesting times. $n = 4$, error bars indicate SD, and ns indicates no significant difference (Student's t-test).

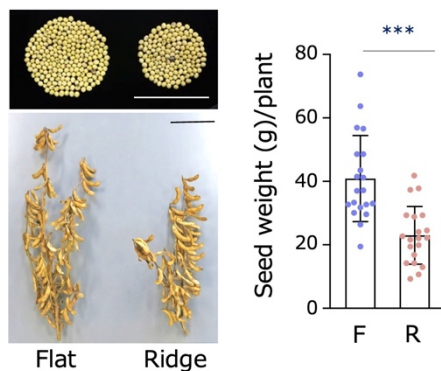


Fig. 2. Soybean growth in the field drought stress experimental system with ridges

Morphology and yield at harvest of soybean grown in this drought stress experimental system. The left side shows the flats (F), and the right side shows the ridges (R). Bars indicate 10 cm in the pictures. $n = 20$, error bars are SD, and asterisks indicate significant differences ($***P < 0.001$, Student's t-test).

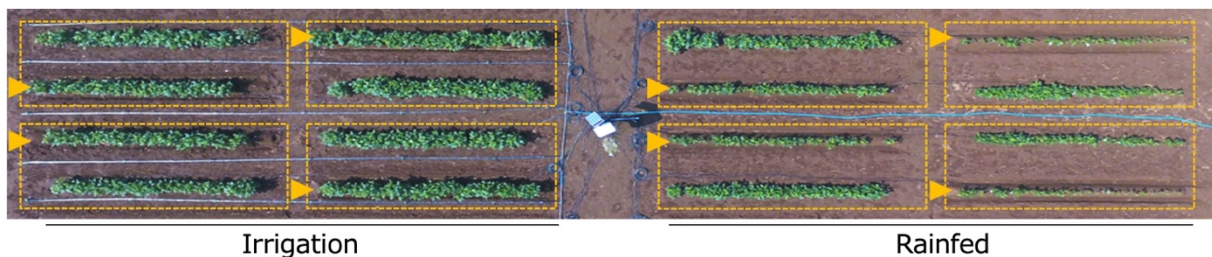


Fig. 3. Irrigation treatment for the field drought stress experimental system with ridges

Growth of soybean about 7 weeks after sowing, taken aerially by drone. Ridges are indicated by yellow arrows. The two rows surrounded by dotted lines indicate one replication including the flat and ridge areas, for a total of four replications of the trial. On the right is the rainfed area (no watering) and on the left is the test area that was irrigated to the same test design as the rainfed area on the right (irrigated area). The white box in the center contains the data loggers connected to the soil moisture sensors inserted in each row.

Reference: Nagatoshi et al. (2023) *Nature Communications* 14: 5047. © The Author(s) 2023. The figures were reprinted/modified from Nagatoshi et al. (2023).

Novel drought stress response mechanisms in plants

Drought is the most serious environmental stress that threatens crop growth and survival. Even a mild drought with no leaf wilting can significantly reduce crop growth and have a profound impact on yields. Therefore, early detection of such "invisible droughts" and appropriate measures such as irrigation are important for stable crop production. However, the response of crops to "invisible drought" in the field and its mechanisms have not been well understood. In this study, using a drought stress evaluation system with ridges we developed, we elucidated the plant response to the "invisible drought" that occurs in the field and its physiological significance through detailed analysis in the laboratory and using model plants.

To understand the plant response to the "invisible drought" that occurs in the field, we conducted RNA sequencing analysis using the leaves of soybean grown on flats and those grown on ridges. The data showed that a battery of phosphate starvation response (PSR) genes was up-regulated under mild drought conditions (Fig. 1). By elemental analysis of the leaves, it was demonstrated that mild drought stress reduces levels of Pi among the three primary macronutrients, N, P, and K, in plants in the field. In addition, we showed that the expression of PSR genes is induced in a soil water-dependent manner during the initial phase of drought stress in soybean grown in pots with controlled soil water contents. Furthermore, as drought stress intensifies, the expression of abscisic acid (ABA) response genes is induced (Fig. 2). Not only in soybean but also in *Arabidopsis thaliana*, the expression of PSR genes is induced in the early phase of drought stress before the expression of ABA response genes is induced, suggesting that the newly found phenomenon is universal in plants. In PSR-deficient *Arabidopsis* mutant plants, growth is significantly suppressed by mild drought stress compared to wild-type plants, suggesting that induction of PSR gene expression under mild drought stress plays an important role in maintaining growth during water stress (Fig. 3).

Phosphate content and expression of PSR genes are expected to contribute to the development of plant water sensors as early indicators of "invisible drought," but it is necessary to consider the possibility that environmental conditions other than soil moisture may also affect the induction of phosphate deficiency responses.

Authors: Nagatoshi, Y., Kobayashi, Y., Fujii, K., Baba, J., Fujita, Y., Ikazaki, K., Oya, T. [JIRCAS], Mizuno, N., Yasui, Y. [Kyoto Univ.], Sugita, Y. [Nagoya Univ.], Takebayashi, Y., Kojima M. [RIKEN], Sakakibara H., [RIKEN & Nagoya Univ.], Kobayashi, I. N., Tanoi, K. [Univ. of Tokyo], Ogiso-Tanaka, E., Ishimoto, M. [NARO]

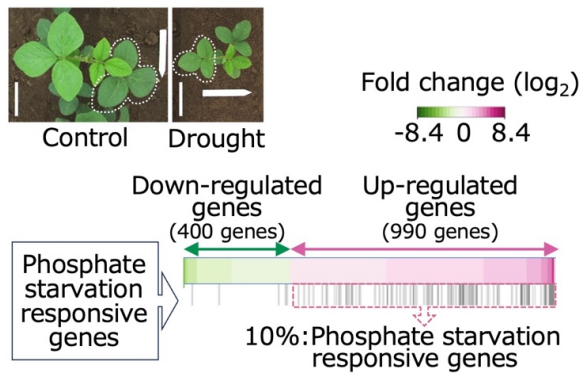


Fig. 1. Induction of PSR genes in soybean leaves under mild drought conditions in the field

Transcriptome analysis of soybean grown in a drought stress evaluation system using ridges in the field. The second leaf of soybean at 31 days after sowing (dotted line in the photo) was used for RNA-seq analysis. Bars in the photo represent 10 cm.

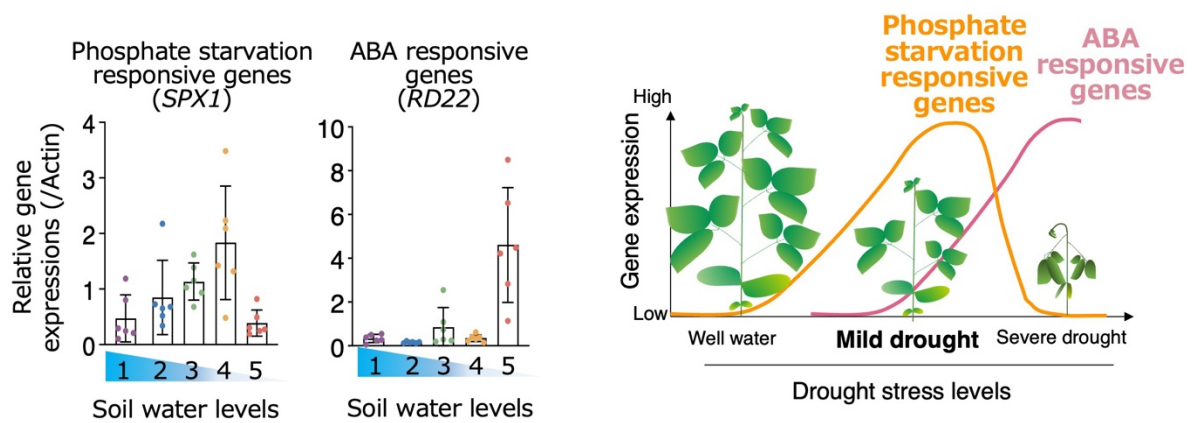


Fig. 2. Expression of PSR genes and ABA-responsive genes induced in a soil water-dependent manner during mild drought

(A) Gene expression analysis of soybean grown in a greenhouse under controlled soil water levels in pots (levels 1-5; higher values indicate less water and greater degree of drought). n = 6, error bars = SD. (B) Model diagram of a newly presented plant drought stress response.

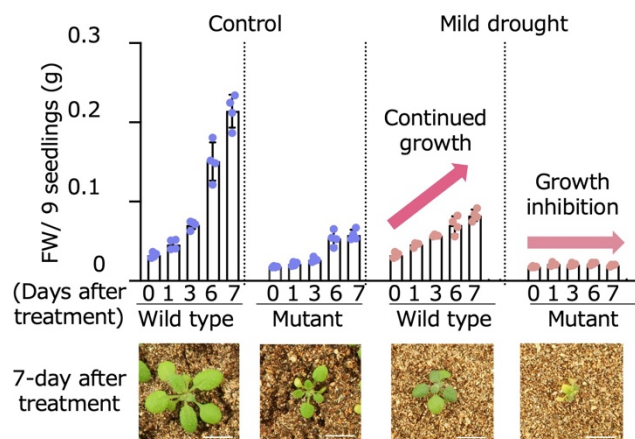


Fig. 3. Drought stress response of *Arabidopsis* PSR-deficit mutants

Growth changes in drought stress-treated *Arabidopsis* wild-type plants and PSR-deficit mutants in which the PSR genes are not induced. Aboveground biomass is shown at 1, 3, 6, and 7 days after drought stress treatment (after water supply to the growing pots was stopped). Bars in the pictures represent 1 cm. n = 4. Error bars indicate SD.

Reference: Nagatoshi et al. (2023) *Nature Communications* 14: 5047. © The Author(s) 2023
The figures were reprinted/modified from Nagatoshi et al. (2023).

Mathematical modeling is an effective approach in predicting the temporary expression pattern of the nitrate transporter gene *NRT2.1*

Nitrogen (N), a constituent of many biomolecules such as nucleic acids and proteins, is an indispensable element for plants. Among the major forms of N, nitrate is prevalent under oxidative environments and its availability is closely related to plant growth. However, excessive nitrate uptake leads to increased energy use and reduced pathogen resistance. Thus, plants fine-tune nitrate uptake by regulating the expression of the gene encoding a major nitrate transporter, *NRT2*. Although it is important to manipulate the expression of *NRT2* to modify N use, intuitively understanding key components for such a modification is difficult, especially when the gene is under a complex regulation. For designing plants with optimized N use and increased resilience, it is important to quantitatively understand the changes in the response caused by changes in the regulatory pattern. This study aimed at elucidating important regulatory factors for *NRT2* by comprehensively analyzing its regulatory system via mathematical modeling.

Temporary changes in the expression of Arabidopsis *NRT2.1* (a member of the *NRT2* family) were fitted to an ordinary differential equation to determine coefficients, and a mathematical model describing the temporary expression pattern of *NRT2.1* and other related molecules was developed (Fig. 1). The model predicted that the absence of negative regulation of *NRT2.1* by NIGT1, a transcriptional repressor, decreases the stability of *NRT2.1* expression under a wide range of activity of NLP, which induces the expression of *NRT2.1* and *NIGT1* genes in the presence of nitrate (Fig. 2). This hypothesis was further validated experimentally using mutant plants lacking the regulatory pathway from NIGT1 to *NRT2.1*; the expression of *NRT2.1* was stable under a wide range of nitrate concentrations in the wild-type plants, whereas the expression of *NRT2.1* was greatly affected by nitrate concentrations in the mutant plants (Fig. 3).

The quantitative description of the temporary response pattern related to N use provides clues on which regulatory component should be altered for a certain desired response. Since a similar regulatory pattern of *NRT2* is conserved in other plant species including rice, this mathematical modeling is likely to be effective in other plant species. This approach is also applicable to other traits and other plant species, especially when the trait is under a complex regulation. This approach is useful for designing plants with favorable traits and accelerating smart breeding. Further understanding of molecular mechanisms and the expansion of more fundamental data will be helpful to accelerate the applicability of this approach.

Authors: Ueda, Y., [JIRCAS],
Yanagisawa, S. [Univ. of Tokyo]

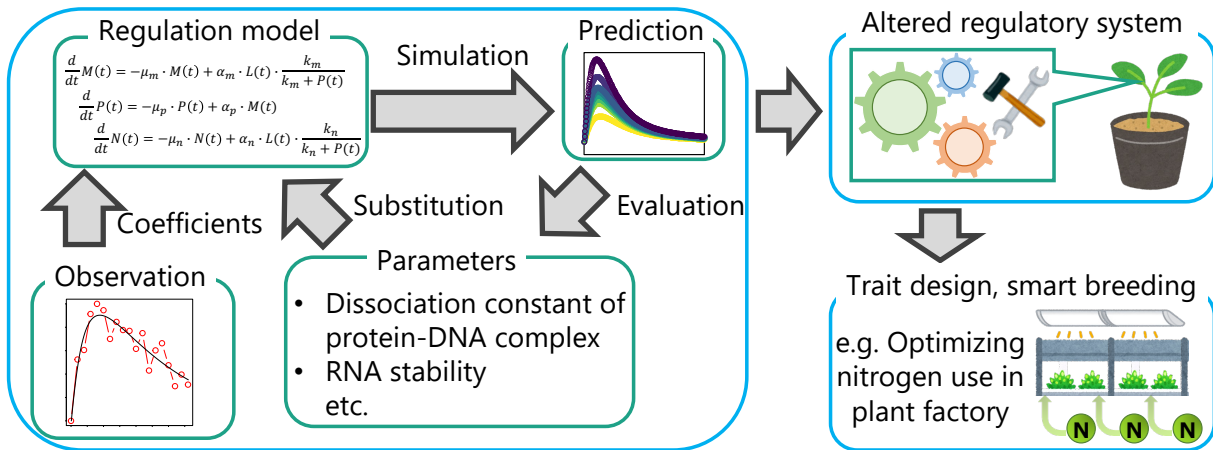


Fig. 1. Concept diagram of the development and use of a mathematical model

Coefficients obtained from experimental data are used to construct the regulation model. The effect of each parameter on the response pattern is evaluated by simulations. The results of simulation shall be used to alter regulatory systems and design crops conferred with a desirable trait.

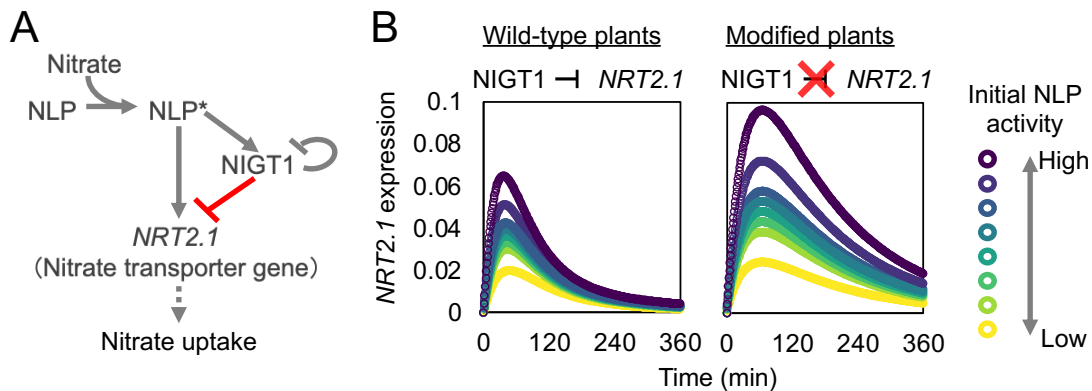


Fig. 2. Regulatory systems involved in nitrate use and prediction of their behavior

(A) Regulatory system involved in nitrate use. Arrow and T sign indicate promotive and suppressive effects, respectively. NLP* indicates activated NLP protein in the presence of nitrate. (B) Predicting the temporary expression pattern of *NRT2.1* in wild-type plants (left panel) and modified plants (right panel) lacking NIGT1 regulation (red sign in A).

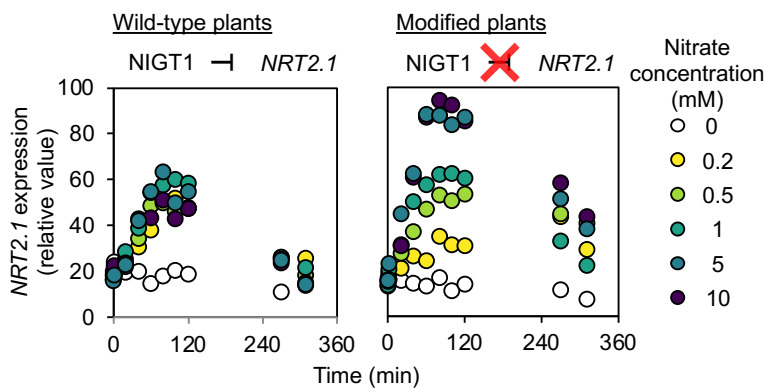


Fig. 3. Experimental validation of the simulation result

Experimentally determined expression levels of *NRT2.1* in the presence of different nitrate concentrations are shown for wild-type plants (left panel) and modified plants (right panel) lacking NIGT1 regulation.

Reference: Ueda and Yanagisawa (2023) *Plant Physiology* 193: 2865–2879. © The Author(s) 2023
The figures were reprinted/modified from Ueda and Yanagisawa (2023).

Optimum phosphorus fertilizer management can balance productivity and quality of black rice

The Southeast Asian region has a rich tradition of utilizing black rice for its medicinal properties. Black rice pericarp contains various secondary metabolites such as anthocyanins, which are known for their antioxidant effects including restoring liver function and preventing dementia. In tropical areas such as Laos, where black rice is commonly consumed, soils typically lack phosphorus (P), an essential nutrient for crops. Therefore, external P supply is crucial to boosting productivity. However, with rising fertilizer costs and the adoption of labor-saving rice cultivation techniques, it is vital to determine the optimal P fertilization levels. Additionally, understanding the impact of P fertilization on flavonoid accumulation, which contributes to antioxidant properties, is necessary. This study aims to conduct pot trials using P-deficient soil to evaluate how soil P availability affects black rice yield and flavonoid content, which serves as an indicator of antioxidant capacity. The goal is to identify the optimal P fertilization strategy to balance productivity and quality in black rice cultivation.

Pot trials conducted on volcanic soils with limited P availability revealed that P fertilization enhances yield up to a certain point but becomes excessive beyond 250 mg P₂O₅ pot⁻¹ (Fig. 1). Exceeding this threshold not only fails to further increase yield but also reduces flavonoid content (Fig. 2) and affects the rice's appearance by lightening its color (Fig. 3). Therefore, P fertilization beyond 250 mg P₂O₅ pot⁻¹ compromises both flavonoid accumulation and appearance traits.

These findings underscore the importance of careful P fertilization management in P-deficient soils. While it boosts black rice yield, excessive fertilization negatively impacts flavonoid content and appearance quality. Thus, adopting proper P fertilizer management practices is essential for producing high-value black rice that maintains a balance between productivity, functionality, and appearance quality. This knowledge can guide cultivation practices tailored to diverse soil conditions in different regions.

Authors: Oo, A.Z., Asai, H., Kawamura, K., Takai, T., Tanaka, J.P., Marui, J., Saito, H. [JIRCAS],
Kawamura, K. [OUVAM], Win, K.T. [NARO]

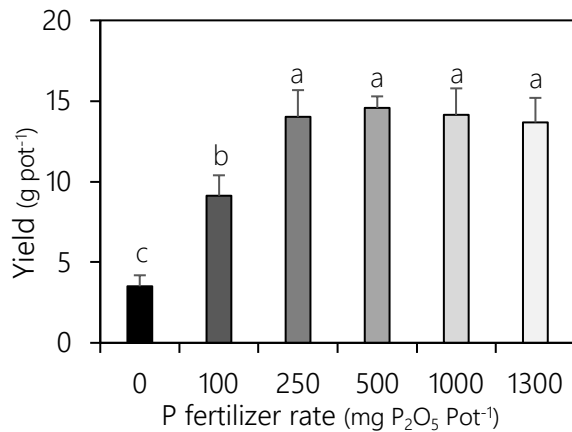


Fig. 1. Yield increases with P application.

Black rice "Asamurasaki" was grown under pot conditions with different amounts of P application rates. Different alphabets indicate significantly different at 5% level (Tukey method, n=5). Error bars in the figure indicate standard deviation.

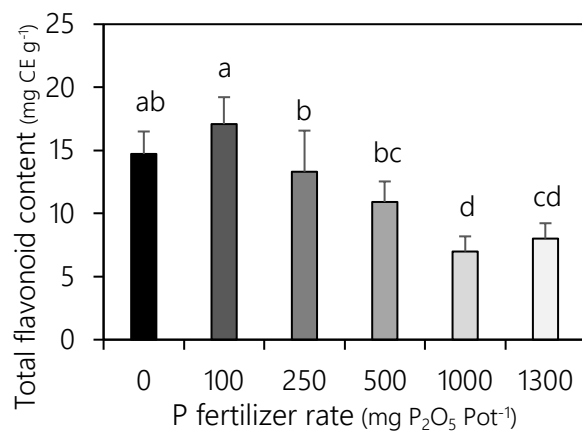


Fig. 2. Total flavonoid content decreases with P application.

Different alphabets indicate significantly different at 5% level (Tukey method, n=5). Error bars in the figure indicate standard deviation.

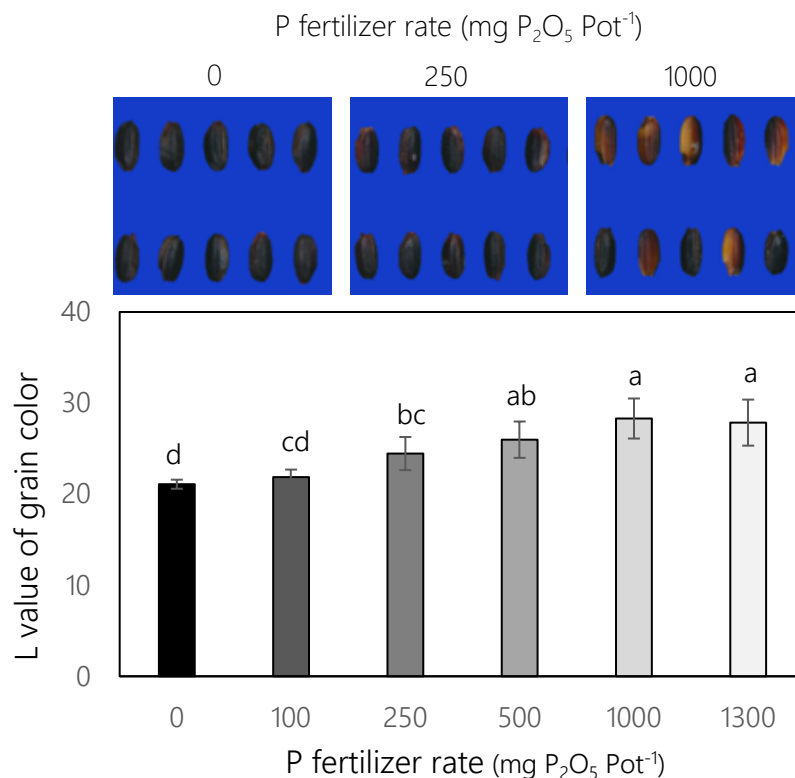


Fig. 3 Lightness of grain color increases with P application.

L value (indicator of lightness) of grain surface was measured with GIE-Lab method. L value close to 100 shows white color and close to 0 shows black color. Different alphabets indicate significantly different at 5% level (Tukey method, n=5). Error bars in the figure indicate standard deviation.

Reference: Oo, et al. (2023) *Frontiers in Sustainable Food Systems* 7: 1200453. © The Authors 2023
The figures were reprinted/modified from Oo et al. (2023).

A simple bioassay method for international comparison of insecticide susceptibility of the fall armyworm, *Spodoptera frugiperda* (J.E. Smith)

The fall armyworm (FAW), *Spodoptera frugiperda*, was a native pest in the Americas (Fig. 1). However, FAW has recently invaded Africa and Asia and is rapidly expanding its distribution. This insect is a polyphagous pest and prefers maize. Due to the frequent use of certain inexpensive and easily available insecticides, resistance development is a concern in Asia. Because of the long-distance migration ability of FAW, if a strain develops resistance to insecticides in one country, it is likely to spread rapidly to neighboring countries. Therefore, it is essential to conduct insecticide susceptibility monitoring using the same methods and share the results to manage insecticide resistance development. For this purpose, we developed a simple insecticide susceptibility testing method using relatively easily available materials to monitor the insecticide susceptibility of FAW in Southeast Asia, including developing regions.

This method can easily evaluate insecticide susceptibility, in contrast to existing methods such as molecular biology techniques and topical application. It consisted of the following procedures: collecting test insects, rearing them with an artificial diet made from relatively easily available materials, and susceptibility testing (Fig. 2). The artificial diet was composed of three fractions (Table 1). By feeding this artificial diet, 1st instar larvae could be raised to pupae (Fig. 3). We conducted diet-overlay bioassays using the 3rd instar larvae within three generations after collection to assess susceptibility. We applied 200 µl of insecticide serially diluted to any multiple using distilled water to 5 ml of artificial feed. After drying, ten 3rd instar larvae were introduced, and the number of dead individuals was counted 72 hours later. From the results obtained, the LC50 value was calculated. We evaluated the susceptibility of the insecticides that are applied in Southeast Asian countries to several FAW populations collected in Thailand using the developed method. The results suggested that the susceptibility of several insecticides decreased over time (Table 2).

The developed method showed enough accuracy and can be used for international comparison to develop resistance management measures. In Thailand, the susceptibility of FAW to several insecticides has decreased. Therefore, there is an urgent need to develop alternative control methods against FAW. The survival rate of 1st and 2nd instar larvae when fed an artificial diet was lower than when fed fresh maize leaves. Thus, fresh leaves are suitable for feeding the young larvae if it is necessary to examine a lot of insecticides in the same period.

Authors: Kobori, K. [JIRCAS], Thirawut, S., Sutjaritthammajariyankun, W., Rukkasikorn, A. Punyawattoe, P., Noonart, U. [Department of Agriculture, Thailand]



Fig. 1. Fall armyworm larva feeding on maize

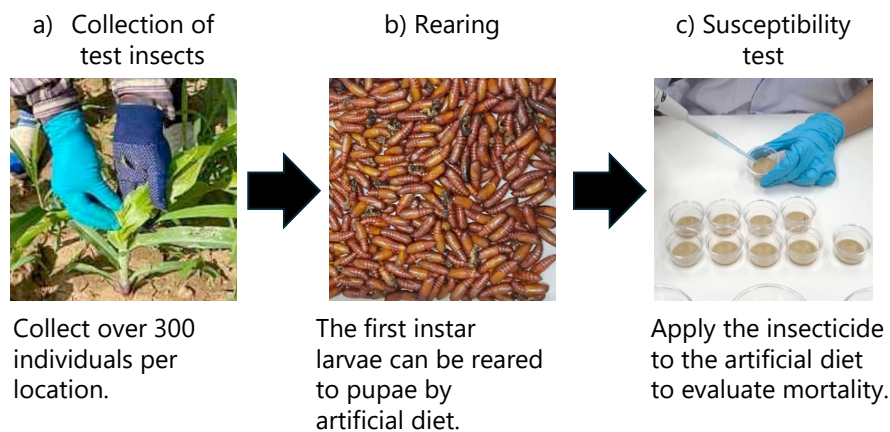


Fig. 2. Summary of the simple insecticide susceptibility test method

Table 1. Composition of the artificial diet

	Ingredients	Quantity
Fraction A	Agar powder	25g
	Reverse osmosis water	800ml
Fraction B	Formalin	4ml
	Yeast	20g
	Methyl paraben	5g
	Sorbic acid	3g
	Mungbean powder	240g
	Reverse osmosis water	800ml
Fraction C	Ascorbic acid (Vitamin C)	5g
	Vitamin stock ¹⁾	40ml

1) Vitamin stock contains 5 mg biotin, 2.5 g thiamine (vitamin B1), 1.5 g pyridoxine (vitamin B6), 3 g riboflavin (vitamin B2), 20 mg cyanocobalamin (vitamin B12), 3 g D-Pantothenic acid hemicalcium salt, 10 g choline chloride, 2.5 g folic acid, 5 g inositol, 6 g nicotinic acid, distilled water 1,000 ml



Fig. 3. FAW pupa reared by artificial diet

Table 2. Results of insecticide susceptibility test of several populations in Thailand

Insecticides	Collected year (Location)	LC50 (mg/L) ¹⁾
Emamectin benzoate 1.92% EC	2019 (Kanchanaburi)	0.014 (0.013–0.016)
	2019 (Tak)	0.015 (0.013–0.018)
	2021 (Suphan Buri)	0.017 (0.014–0.025)
	2021 (Lop Buri)	0.029 (0.023–0.039)
	2022 (Loei)	0.027 (0.021–0.036)
Indoxacarb 15% EC	2019 (Kanchanaburi)	1.526 (0.982–2.048)
	2019 (Tak)	1.877 (1.402–2.337)
	2021 (Lop Buri)	5.259 (3.554–9.019)
	2022 (Sa Kaeo)	7.530 (5.772–10.645)
	2022 (Loei)	10.466 (7.909–15.650)
Chlorfenapyr 10% SC	2019 (Kanchanaburi)	2.086 (1.268–3.450)
	2019 (Tak)	2.049 (1.243–3.360)
	2021 (Lop Buri)	7.056 (6.120–8.122)
	2022 (Sa Kaeo)	7.733 (6.714–8.915)
	2022 (Loei)	8.874 (7.669–10.284)

Reference: Thirawut et al. (2023) *CABI Agriculture and Bioscience* 4: 19. © The Author(s) 2023
<https://doi.org/10.1186/s43170-023-00160-8>
 Figures and tables reprinted/modified from Thirawut et al. (2023).

A quantitative locus, *MP3*, which increases panicle number, enhances grain yield under an elevated atmospheric CO₂ environment

The atmospheric concentration of CO₂, one of the greenhouse gases, is projected to reach 430–1,000 ppm by the end of this century, increasing the average global temperature by 1.0–5.7°C above pre-industrial levels (1850~1900). While the increase in temperature will have a negative effect on crop productivity in some regions, the increase in atmospheric CO₂ concentration will have a positive effect on plant photosynthesis. Therefore, crops with sufficient spikelets to store increased photosynthetic assimilates are expected to contribute to increased yield, and the utilization of such crops under high CO₂ concentrations may lead to sustainable crop production under climate change. We have previously shown that a quantitative locus, *MP3* (*MORE PANICLES 3*), found in the temperate *japonica* rice cultivar Koshihikari, promotes tillering and increases panicle number in the high-yielding *indica* cultivar Takanari. The purpose of this study is to identify the causal gene of *MP3* by map-based cloning, clarify the rice groups in which *MP3* is effective, and verify that increased panicle number due to *MP3* contributes to increased grain yield under an elevated atmospheric CO₂ environment.

We can see the results of map-based cloning in Fig. 1. The causal gene of *MP3* is *OsTB1* (*TEOSINTE BRANCHED1*) located on chromosome 3, and there are three sequence differences in the gene between Koshihikari and Takanari. Classifying rice cultivar groups based on the sequence differences, 74% of temperate *japonica* cultivars and 10% of tropical *japonica* cultivars have the same sequence as Koshihikari (Koshihikari type). On the other hand, 60% of the *indica* cultivars have the same sequence as Takanari (Takanari type) (Fig. 2). Then, near-isogenic lines (NILs) carrying the Koshihikari *MP3* in the high-yielding *indica* cultivars, IR64 and Hokuriku 193, also increase panicle number by 20–30% compared to the parental cultivars as in the case of Takanari (Fig. 3). Interestingly, Takanari-NIL enhances grain yield by 6% compared to Takanari under open-air CO₂ enrichment (FACE, 580 ppm CO₂ in the air), whereas it does not under ambient condition (390 ppm CO₂ in the air) (Fig. 4).

Since *indica* cultivars are grown on more than 80% of the world's rice cropping areas, the Koshihikari *MP3* is expected to be widely used in rice breeding in Japan and abroad to address climate change accompanied by rising atmospheric CO₂ levels. However, it should be noted that the effect of *MP3* on panicle number and grain yield under high-temperature conditions needs to be verified in the future.

Authors: Takai, T., Tsujimoto, Y., Asai, H., Kawamura, K., Maruyama, K., Ishizaki, T. I., Kobayashi, N. [JIRCAS], Taniguchi, Y., Takahashi, M., Hirose, S., Hara, N., Sanoh-Arai, Y., Hori, K., Fukuoka, S., Sakai, H., Tokida, T., Usui, Y., Kondo, M., Hasegawa, T., Uga, Y. [NARO], Akashi, H., Ito, J., Tsuji, H. [Yokohama City Univ.], Mochida, K. [RIKEN], Yamamoto, E. [Meiji Univ.], Nagasaki, H. [Kazusa DNA], Nakamura, H. [Taiyo Keiki]

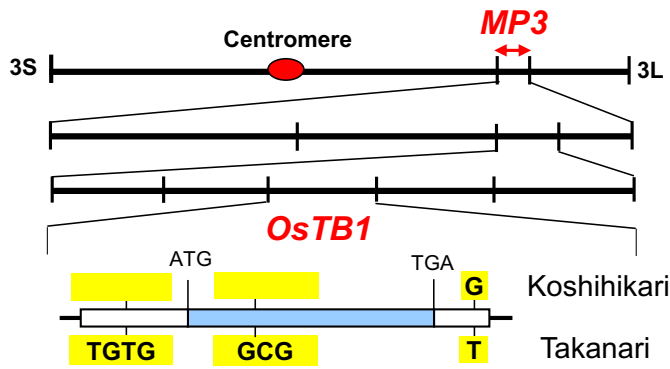


Fig. 1. Map-based cloning of *MP3*

Sequence differences exist in the three locations highlighted in yellow. Blank yellow indicates that the corresponding sequence is deleted.

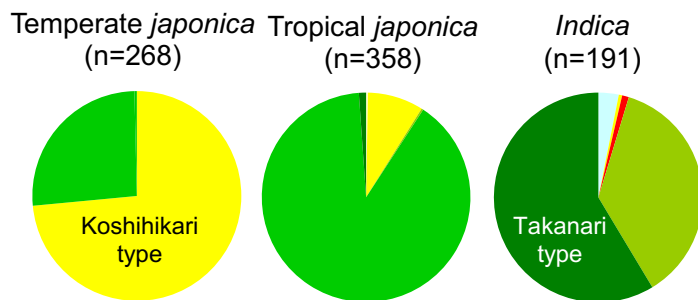


Fig. 2. Type of *MP3* among temperate *japonica*, tropical *japonica*, and *indica*

n means the number of cultivars.

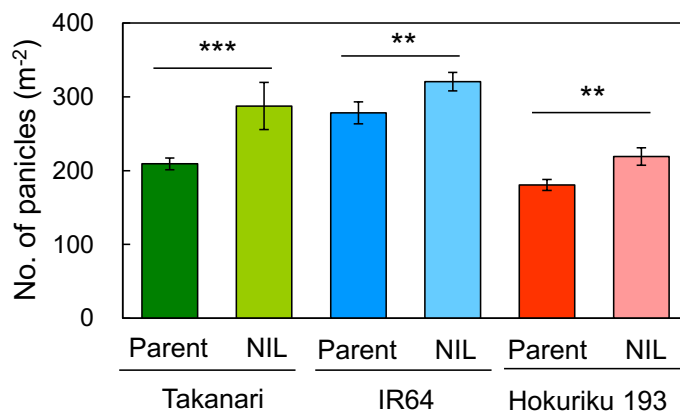


Fig. 3. Comparisons of panicle number between the parental cultivars and its near-isogenic lines (NILs)

*** and ** show significance at 0.1% and 1% levels, respectively.

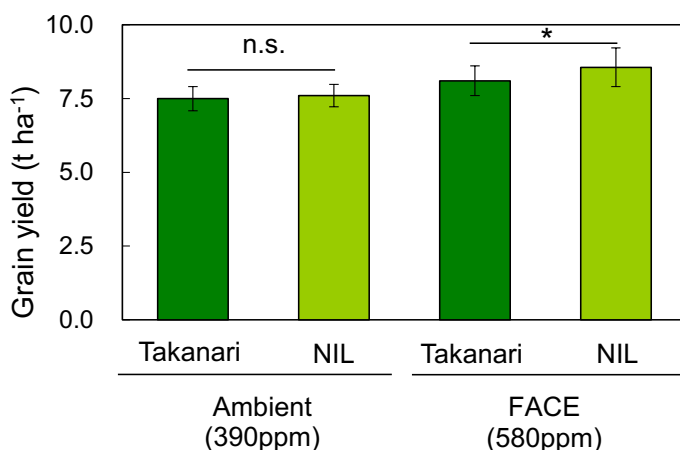


Fig. 4. Comparisons of grain yield between Takanari and its NIL grown in ambient CO₂ and open-air CO₂ enrichment (FACE) conditions

n.s. and * show non-significance and significance at 5% levels, respectively.

Reference: Takai et al. (2023) *The Plant Journal* 114: 729–742. © The Author(s) 2023
The figures were reprinted/modified from Takai et al. (2023).

Weakening of gene function of *OstB1* by genome editing improves rice productivity under phosphorus deficiency

Tillering is an important trait that determines shoot architecture and yield in rice. Many genes are involved in tillering in rice, and among them, rice *TEOSINTE BRANCHED1* (*OstB1*) is a key gene that suppresses tillering. On the other hand, phosphorus, a soil nutrient, is one of the most important environmental factors involved in tillering. Phosphorus deficiency leads to reduced tiller number and is a major constraint on rice production in sub-Saharan Africa. In this study, we generate mutants for *OstB1* using the CRISPR/Cas9 system in X265, which is a major rice cultivar in Madagascar, and then investigate tillering and productivity under phosphorus deficiency in the resultant mutants.

The CRISPR/Cas9 system has generated two types of mutant lines: an in-frame mutant line with 30-bp deletion (#29418) and a frameshift mutant line with 1-bp insertion (#29430) (Fig. 1). The in-frame mutant line #29418 has 1.2 times more tillers than the background cultivar X265 (WT) at just before heading stage (Fig. 1). On the other hand, the frameshift mutant line #29430 produces 3.4 times more tillers than WT (Fig. 1). This means that *OstB1* weakens its tillering suppression function through the in-frame mutation, while the frameshift mutation loses its tillering suppression function. The expression level of the *OstB1* gene in #29418 is comparable to that of WT (Fig. 2). The *OstGT1* gene, which is directly regulated by *OstB1* to suppress tillering, is down-regulated in #29430 (Fig. 2). The expression level of *OstGT1* in #29418 is intermediate between those of WT and #29430 (Fig. 2), revealing that the modified *OstB1* expressed in the in-frame mutant line #29418 has a moderate function in the regulation of *OstGT1*. The grain yield of #29418 under phosphorus deficiency is higher than that of WT under low phosphorus application levels: #29418 has approximately 40% higher grain yield than WT under 0 mg/kg phosphorus application (Fig. 3A). The number of panicles, spikelets, and filled grains of #29418 was higher than those of WT, and the 1,000-grain weight was lower than that of WT (Fig. 3B). The gain in filled grain numbers more than compensates for the reduced 1,000-grain weight. On the other hand, the frameshift mutant line #29430 has more filled grains than WT, but it does not improve yields because the gain in filled grain numbers does not compensate for its decreased 1,000-grain weight.

Our study demonstrates that genome editing of *OstB1* can modify tillering in rice and suggests that the breeding of rice cultivars that have a moderately higher number of tillers may effectively improve rice productivity in areas suffering from phosphorus deficiency.

Authors: Ishizaki, T., Ueda, Y., Takai, T., Tsujimoto, Y., Maruyama, K. [JIRCAS]

Line	Sequence of target site	Insertion/deletion
WT	CCGCTCACGGCCACAGCGACGGG	
#29418	C-----	30 bp deletion
#29430	CCGCTCACGGCCACAGCTGACGGG	1 bp insertion

Fig. 1. Generation of mutants for *OsTB1* by genome editing

(A) DNA sequences of mutated *OsTB1* generated by CRISPR/Cas9. Underlines in the target sequences indicate PAM. A red letter indicates an inserted nucleotide. Red dashes indicate deleted nucleotides. (B) Plants of WT (left), #29418 (in-frame mutant; center), and #29430 (frameshift mutant) at just before heading stage. The mean tiller numbers of each line are indicated at the bottom of pictures.

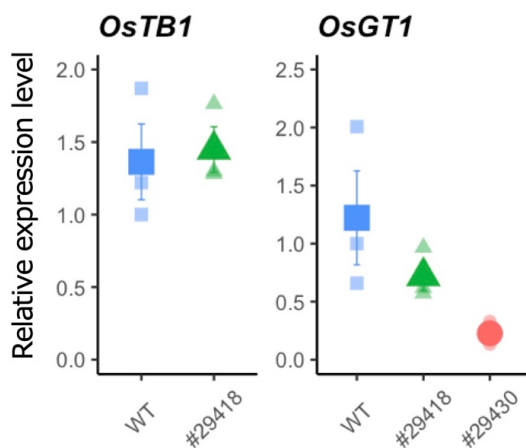


Fig. 2. Expression analysis of *OsTB1* and *OsGT1*

Expression levels in the basal node region of 21-day-old plants are quantified by qRT-PCR. *OsGT1* is a gene that *OsTB1* directly binds to its promoter to induce its expression. Each large symbol represents the mean from three biological replications, and each small symbol represents the observed raw value for each replication. #29418, in-frame mutant; #29430, frameshift mutant.

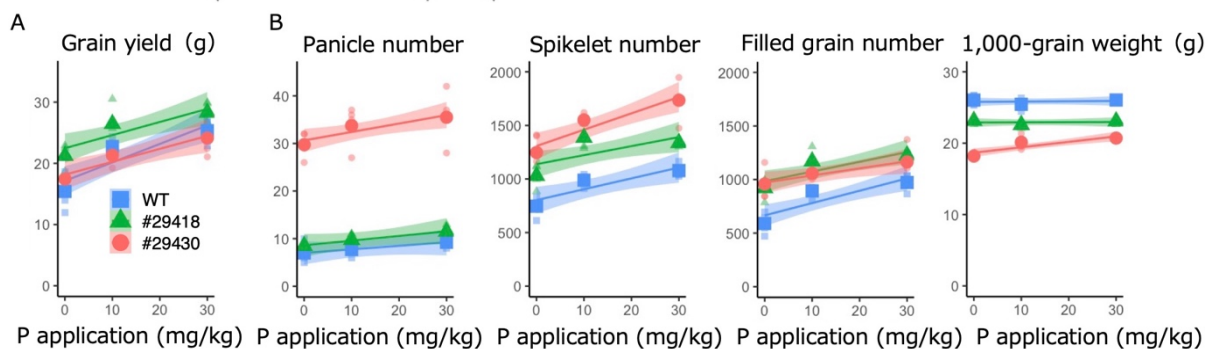


Fig. 3. Grain yield and yield components of mutants for *OsTB1* under different phosphorus (P) applications

#29418 (in-frame mutant), #29430 (frameshift mutant), and WT (X265) were grown in soil supplemented with 0, 10, or 30 mg/kg of P until the mature stage. (A) Grain yield per plant. (B) Yield components of the in-frame mutant line (#29418) and non-mutated X265 (WT). Each large symbol represents the mean from four replications, and each small symbol represents the observed raw value for each replication. Predictions and 95% confidence intervals by ANCOVA are indicated respectively with lines and shading.

Reference: Ishizaki et al. (2023) *Plant Science* 330: 111627. © The Author(s) 2023
The figures were reprinted/modified from Ishizaki et al. (2023).

A simple method for estimating phosphorus (P) retention capacity in paddy soils based on soil moisture content: An effective approach for P fertilization diagnosis

Soils possess the inherent ability to adsorb phosphorus (P), known as P retention capacity. When this capacity is high, the effectiveness of P fertilizer application diminishes. This issue is particularly pertinent in sub-Saharan African (SSA) farmlands, where soil P content is low and farmers have limited access to fertilizers. Effective application of P fertilizers becomes crucial to increasing crop yields in such contexts. Understanding the variability of soil P retention capacity, even among neighboring fields, is essential before fertilizer application. However, analyzing soil P retention capacity typically involves hazardous reagents and expensive equipment, making widespread implementation challenging especially in SSA research institutions with insufficient analytical facilities. In a previous study, we found a significant correlation between the active aluminum content, which determines soil P retention capacity, and the moisture content of air-dried soil in neutral to acidic soils. Yet, the instability of moisture content due to changes in humidity during air drying caused measurement errors. Hence, this study aimed to develop a method to estimate soil P retention capacity accurately and easily by employing saturated salt solution as a moisture conditioning agent to regulate soil moisture content.

The study examined 306 surface soil samples from lowland rice fields in Madagascar, representing diverse soil properties with soil P retention capacity ranging from 10.1% to 96.1%. The results demonstrate that P retention capacity can be accurately estimated based on soil moisture content (Fig. 1). Soil moisture content was measured based on the weight changes before and after exposure to saturated salt solution for one week, which requires no chemical analysis (Fig. 2). By placing saturated salt solution (wherein at least 36 g of sodium chloride is dissolved in 100 g of water) as a moisture conditioning agent inside a closed container for soil placement, regardless of variations in the initial dryness before placement and the relative humidity outside the closed container, soil moisture content can be measured with high reproducibility (Fig. 3). These findings provide practical utility for agricultural extension officers to identify fields responsive to P fertilization with low P retention capacity, facilitating prioritized P fertilizer application for optimal crop yield. While this method is applicable to common lowland rice fields in tropical and subtropical regions, caution is advised for soils with high pH and exchangeable cation content, necessitating thorough validation before implementation.

Authors: Nishigaki, T., Tsujimoto, Y. [JIRCAS],
Andriamananjara, A., Rakotonindrina, H. [Univ. of Antananarivo]

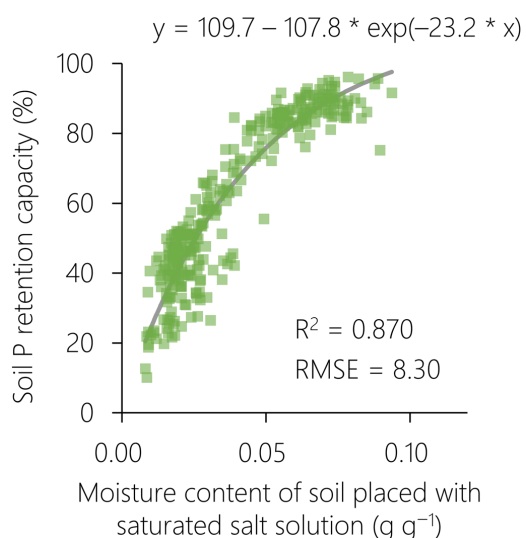
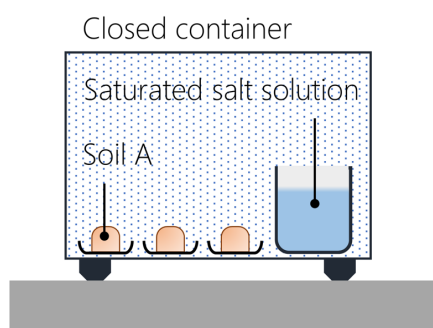


Fig. 1. Relationship between moisture content and P retention capacity of soils placed with saturated salt solution

Coefficient of determination (R^2): It indicates how closely the predicted values match the actual values, with a value closer to 1 indicating higher accuracy.

Root Mean Square Error (RMSE): It represents the average square root of the squared differences between predicted values and actual values, indicating that smaller values suggest a model with lower error.



Moisture content of Soil A ($g\ g^{-1}$)

$$= \frac{\text{Weight of Soil A after placing with saturated salt solution (g)} - \text{Weight of Soil A after oven-drying (g)}}{\text{Weight of Soil A after oven-drying (g)}}$$

Fig. 2. Overview of placing soil with saturated salt solution in a closed container and the formula for calculating soil moisture content

Saturated salt solution (saturated sodium chloride (NaCl) solution) is used as a moisture conditioning agent. Saturated NaCl solution is known to maintain relative humidity nearly constant within the range of room temperature with minimal influence from temperature. When using approximately one cup of soil (about 200 g), weight is measured using an electronic balance capable of measuring up to 0.1 g.

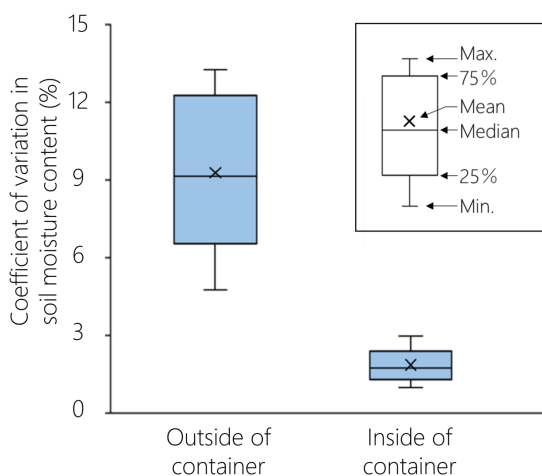


Fig. 3. The coefficient of variation of soil moisture content after placing various soils outside and inside of closed container under different relative humidity conditions

A box plot of the coefficient of variation of soil moisture content after one week of placement of various soils ($n = 20$, P retention capacity 19.6–94.1%) outside and inside of a closed container at relative humidities of 41%, 52%, and 64% (all at 20°C).

Reference: Nishigaki et al. (2023) *Soil Science and Plant Nutrition* 69: 337–345.
 © Japanese Society of Soil Science and Plant Nutrition 2023
 Figures reprinted/modified from Nishigaki et al. (2023) with permission.

Localized phosphorus application via P-dipping is effective in avoiding flooding damage for lowland rice production

To achieve higher production with minimal environmental impact in sub-Saharan Africa (SSA), it is crucial to make technical transitions from low-input to nutrient-use-efficient production systems. P-dipping, a localized phosphorus (P) application on seedling roots, is a potential approach to enable such a transition for lowland rice production. However, empirical evidence on the effectiveness of this approach in smallholders' heterogeneous field conditions is lacking. Therefore, 18 on-farm trials were implemented by applying three P application treatments (zero P; P broadcast at 13.1 kg P ha⁻¹; P-dipping at 13.1 kg P ha⁻¹) with and without N top-dressing (60 kg N ha⁻¹) under a range of topographic, edaphic, and climatic conditions in the highlands of Madagascar.

The P-dipping method had greater yields, exceeding by 1.1 t ha⁻¹ vs. zero P and by 0.5 t ha⁻¹ vs. P broadcast on average under the non-N-applied condition. The yield advantage of P-dipping was enlarged with N application, and thus, the effect of N on grain yield was greater in P-dipping than in zero P or P broadcast (Fig. 1). The P-dipping effect was increased when the fields had erratic water levels after transplanting, which was associated with vigorous initial growth and avoidance of submergence stress (Fig. 2). Multiple regression analysis detected that the effect of P-dipping on grain yield was prominent not only in fields with initial submergence stress but also in fields at high elevation/cool climate site and late-transplanted fields at low elevation/warm climate site where P-dipping alleviated late-season low-temperature stress by shortening days to heading (Fig. 3). This study revealed that the effect of P-dipping is consistent in various P-deficient soils and is enhanced by combining with N topdressing and when fields are prone to late-season cold stress or early-season submergence stress. The results of this study show that P-dipping has the potential to improve fertilizer use efficiency and help farmers cope with frequent flooding. The technology is expected to contribute to stable and sustainable rice production in sub-Saharan Africa as its use expands.

Authors: Oo, A.Z., Tsujimoto, Y. [JIRCAS],
Rakotoarison, N. [FOFIFA], Andranary, B. [University of Antananarivo]

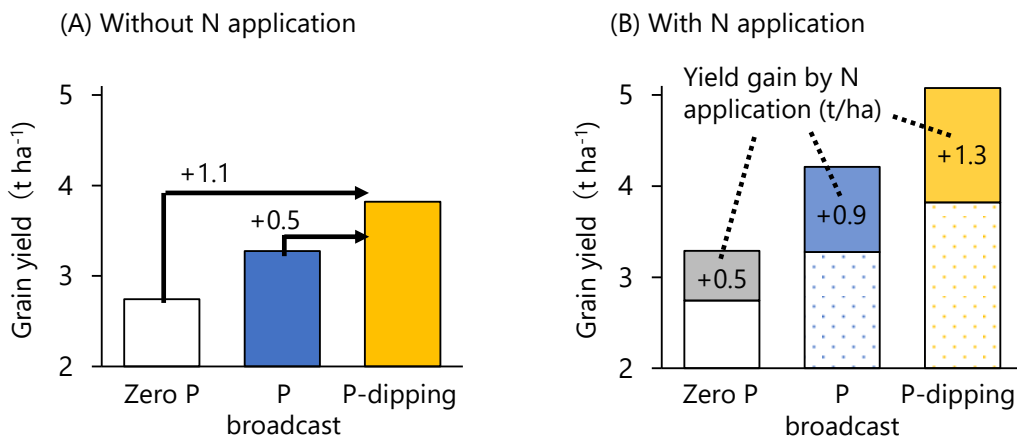


Fig. 1. Yield gain by P-dipping without N (A) and with N application (B)

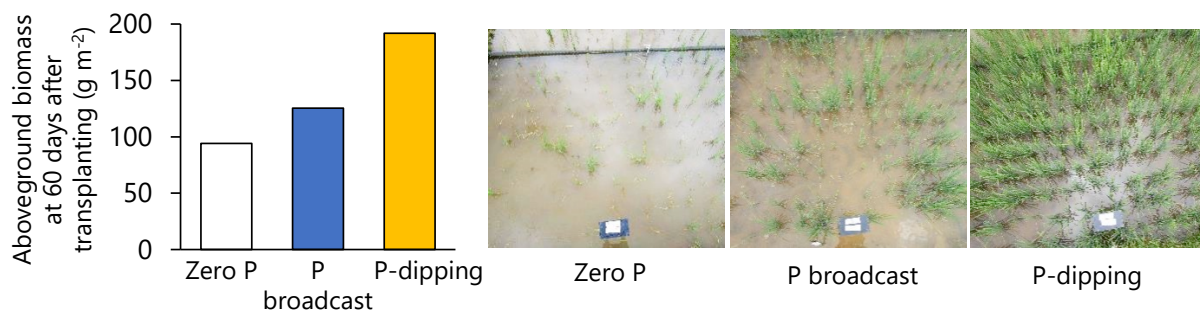


Fig. 2. Effect of P-dipping on the aboveground biomass at 60 days after transplanting and on submergence stress avoidance

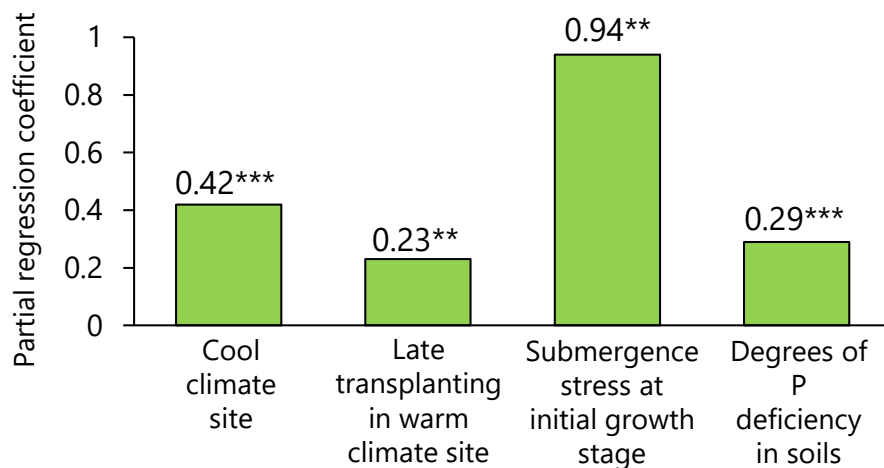


Fig. 3. Determinant factors with their partial regression coefficients for the field-to-field variations in the P-dipping effect on rice yield

Reference: Oo et al. (2023) Localized phosphorus application via P-dipping doubles applied P use efficiency and avoids weather-induced stresses for rice production on P-deficient lowlands. *European Journal of Agronomy* 149: 126901. © Elsevier B.V. 2023
The figures were reprinted/modified from Oo et al. (2023) with permission.

Localized phosphorus application via P-dipping is most effective in increasing lowland rice yields when combined with seedlings at 4.5~6.5 leaf age

P-dipping refers to the placement of phosphorus (P) fertilizer at the root system during transplanting of rice by adhering P-enriched slurry to the seedling roots. This approach is beneficial for smallholder farmers in sub-Saharan Africa who apply small amounts of P to highly P-fixing soils. This study aimed to identify the optimum seedling age for maximizing the impact of P-dipping. Pot experiments revealed that the adhered amounts of slurry to the roots with P-dipping increased in a sigmoidal pattern against seedling age along with the increases in the root mass (Fig. 1). Correspondingly, the effect of P-dipping on the initial biomass was enlarged with older seedlings in a sigmoidal pattern, increasing slowly during the young seedling age (<4.5 leaves), sharply during the intermediate seedling age, and plateauing during the old seedling age (>6.5 leaves) (Fig. 2). Combining P-dipping with much older seedlings at 8 leaves resulted in severe transplanting shock and plant death.

On-farm trials on 90 fields demonstrated a significant interaction between seedling age and P treatment on grain yield under a range of growing conditions in the central highlands of Madagascar. The highest yield gains over the control from P-dipping were observed in seedlings with intermediate age (4.5~6.5 leaves), followed by old (>6.5 leaves) and young (<4.5 leaves) seedlings at 1.0 t ha⁻¹, 0.7 t ha⁻¹, and 0.6 t ha⁻¹, respectively (Table 1). These results suggested that vigorous and intermediate seedlings with higher slurry adherence than young seedlings and a lower risk of transplanting shock than old seedlings benefited most from P-dipping (Fig. 3). This finding provides smallholder farmers with practical knowledge on how to apply P-dipping more efficiently for achieving improved P management for sustainable rice production. It should be noted that the optimal seedling status and root development for P-dipping can be affected not only by the leaf age but also by the growth conditions in the nursery bed, e.g., sowing density, temperature, water management, light intensity, soil fertility, fertilizer management, and varieties.

Authors: Tsujimoto, Y., Oo, A.Z. [JIRCAS],
Rakotoarison, N. [FOFIFA], Tashiro T., Kano, M., Ehara, H. [Nagoya University]

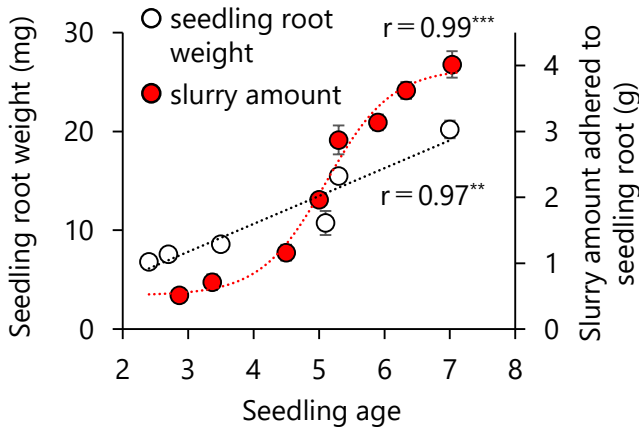


Fig. 1. Relationship between seedling age and (A) root weight and (B) slurry amount adhered to root

Seedlings were raised in a growth chamber at 25°C /15°C day/night temperature and at 20,000 lx.

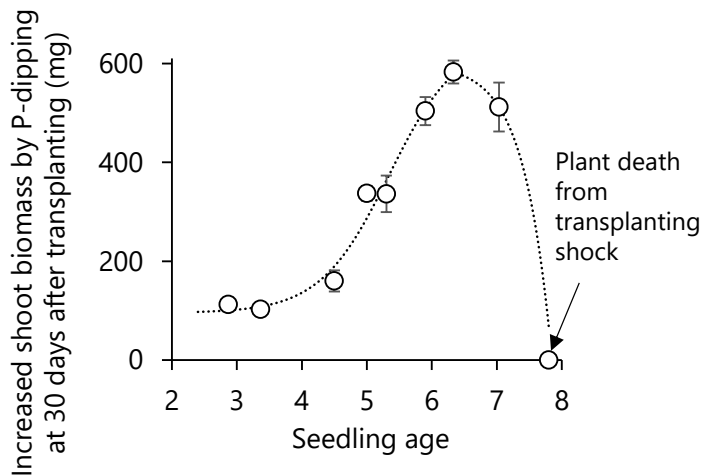


Fig. 2. Effect of P-dipping on initial biomass production using different seedling age

Plants were grown in a growth chamber at 25°C/15°C day/night temperature and at 20,000 lx.

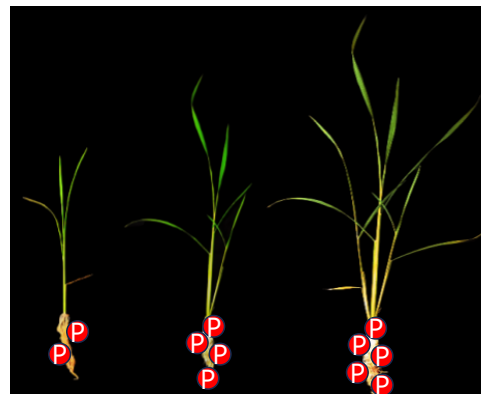
Table 1. Variations in P-dipping effect among farmers' fields using different seedling age in Madagascar

Seedling age at transplant	Number of days in nursery (standard deviation)	Number of farmer fields	P-dipping	Grain yield (t ha ⁻¹)	Yield gain by P-dipping (t ha ⁻¹)
< 4.5	26 (6)	36	No	2.9 b	-
			Yes	3.5 a	0.6 b
4.5~6.5	47 (6)	37	No	3.0 b	-
			Yes	4.0 a	1.0 a [†]
> 6.5	58 (7)	17	No	2.3 c	-
			Yes	3.0 b	0.7 ab [†]

Means with different alphabets indicate significant differences by Tukey's HSD test. [†]P=0.09.

Apart from the P treatments, farmers used their own preferred varieties and management practices in the establishment of seedlings and transplanting patterns.

> 4.5 leaf age 4.5~6.5 leaf age > 6.5 leaf age



Small ← Adhered amounts of P-slurry → Large

Low ← Risk of salt stress → High

Small Large Small

Effect of P-dipping on yield

Fig. 3. Diagram on the interaction of P-dipping and seedling age

Reference: Rakotoarisoa et al. (2023) *Crop and Environment* 2: 202-208. © The Author(s) 2023
The figures were reprinted/modified from Rakotoarisoa et al. (2023).

Unique fertilizer response of sorghum on Plinthosols with thin effective soil depth

Increasing agricultural productivity is essential to meet the rapidly increasing demand for food in Sub-Saharan Africa (SSA). According to statistics from the FAO, while the population of the region tripled between 1980 and 2020, the productivity per unit area of sorghum, the main grain of semi-arid regions in SSA, increased by only 20% and remains stagnant. To address this problem, West Africa is currently redeveloping its cultivation guidelines, which take account of agro-ecological zones reflecting climate, but not soil type differences. However, a special soil type called Plinthosols, in which the effective soil depth (ESD) is less than 50 cm, is widely distributed in the semi-arid regions of West Africa. Because these soils have lower water-holding capacity than other soil types, the response of sorghum to fertilizer application may differ on the Plinthosols.

Therefore, this study aims to determine the differences in fertilizer response of sorghum on three dominant soil types in semi-arid West Africa: Lixisol (LX), which has a thick ESD of about 100 cm and high water-holding capacity; Plinthosol (PT), which has an ESD of about 50 cm; and Plinthosol (PX), which has an ESD of about 25 cm (Fig. 1).

In a year with 21% (1.3 times the standard deviation) less rainfall than the average year, yields are not reduced in LX, but are reduced in PT and PX (Table 1A). This indicates that lack of soil moisture can limit yield in any of the Plinthosols, suggesting that the optimal sorghum variety (e.g., earlier maturing) and sowing density (e.g., more sparsely planted) may be different in Plinthosols than in Lixisols. The optimal nitrogen (N) application rate for sorghum is 74 kgN ha⁻¹ in LX and PT but 37 kgN ha⁻¹ in PX. The reason for this probably is that the PX with 25-cm ESD has a very limited water-holding capacity and is unable to meet the increased water requirements that accompany the vigorous growth of sorghum with fertilizer application. Since the fertilizer response of sorghum varies greatly among LX, PT, and PX, it is necessary to distinguish between LX, PT, and PX and consider optimal fertilizer amounts, varieties, and seeding densities in the guidelines currently being redeveloped for cultivation in West Africa. This would pave the way for the development of tailor-made cultivation guidelines that will allow farmers to maximize fertilizer application efficiency. Finally, we would like to mention that soil types can be easily determined by ground-penetrating radar in semi-arid West Africa. (For more information, refer to Research Highlight A04 in FY 2018, "Ground-penetrating radar can predict the soil depth at which the petroplinthic horizon starts in the Sudan Savanna, West Africa").

Authors: Ikazaki, K., Nagumo, F. [JIRCAS],
Simporé, S., Barro, A. [INERA]

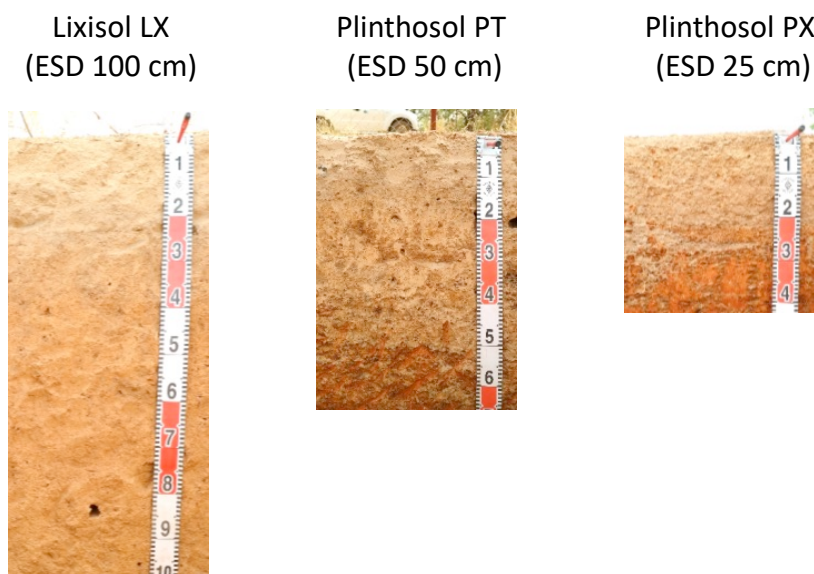


Fig. 1. Soil profiles of the three dominant soil types in the semi-arid West Africa

In PT and PX, an iron hardpan called petroplinthite, which does not allow crop roots to elongate, appears at a depth of about 50 cm and 25 cm, respectively, so the sorghum can only use the water in the soil layer above the iron hardpan.

Table 1. Effects of rainfall amount and fertilization on sorghum yield (kg/ha) in each soil type

	Soil Type		
	Lixisol LX (ESD ¹⁾ 100 cm)	Plinthosol PT (ESD 50 cm)	Plinthosol PX (ESD 50 cm)
A: Rainfall amount	ns ²⁾	*	**
B: Nitrogen application rate ³⁾			
0 kg/ha	522 (52)c	325 (60)c	287 (71)b
37 kg/ha	1040 (121)b	520 (144)bc	800 (79)a
74 kg/ha	1534 (120)a	971 (107)a	808 (105)a
111 kg/ha	1596 (142)a	784 (101)ab	780 (116)a

Results of a 2-year experiment (average and low rainfall years) in central Burkina Faso, where the geology, topography, and soils are representative of semi-arid West Africa. ¹⁾ Effective soil depth.

²⁾ Statistical analysis. ns: not significant ($p > 0.05$), * $p < 0.05$, ** $p < 0.01$; Numbers in brackets are standard errors. Different alphabets indicate that sorghum yields differed significantly ($p < 0.05$) among the same soil type with different nitrogen application rates. ³⁾ Nitrogen was simultaneously applied with phosphorus (23 kg P_2O_5 /ha) and potassium (14 kg/ha).

References: Ikazaki et al. (2023) *Soil Science and Plant Nutrition* 70: 114–122. © The Author(s) 2023
Iseki et al. (2021) *Field Crop Research* 261: 108012. © The Author(s) 2020
Figure and table reprinted/modified from Iseki et al. (2021) and Ikazaki et al. (2023), respectively.

Boosting cowpea grain yield in Plinthosols through fertilization and high plant density

Cowpea cultivation is widespread in the semi-arid regions of West Africa (Sudan Savanna) due to its drought tolerance. Cowpea serves as an important protein source for local farmers; however, due to low soil fertility, the yield per unit area is approximately one-fourth of that in Asia and the United States. The simplest way to increase yield in low-nutrient soils is through fertilization. However, due to high fertilizer costs and limited yield increase even with fertilization, most farmers in the region do not use much fertilizer for cowpea cultivation. Additionally, to compensate for low growth due to limited nutrients, increasing planting density is also considered, but the recommended planting density set over 50 years ago in the region remains unchanged.

Two dominant soil types play a significant role in agricultural productivity in the Sudan Savanna: Lixisols and Plinthosols. Lixisols are relatively fertile with high water retention, but they are prone to waterlogging after rainfall. Plinthosols have low fertility and water retention, with a higher risk of nutrient leaching after rainfall. The objective is to clarify the effects of fertilization and high plant density on these two different soil types to explore cultivation strategies to increase cowpea yields.

The effect of fertilization on yield was approximately 1.4 times higher in Plinthosols compared to Lixisols on average (Fig. 1). This difference is attributed to the high water retention in Lixisols, leading to a temporary decrease in soil oxygen levels and subsequent inhibition of root development due to elevated soil temperature (Fig. 2). Doubling the plant density from the recommended rate resulted in 1.5 times increase in yield in Plinthosols without fertilization, while the increase in yield was smaller in Lixisols (Fig. 1). Combining fertilization and high plant density resulted in higher yield increases than fertilization alone in both soil types (Fig. 1). Splitting fertilization into basal and top-dressing applications also yielded higher than applying all fertilizers at once as basal dressing (Fig. 1).

Soil types vary within a few hundred meters, allowing farmers to efficiently improve cowpea yields by adjusting fertilization rates and planting densities based on soil type within their fields. The ideal timing for top-dressing is around the 4th week after sowing during the maximum vegetative growth period. However, in the Sudan Savanna, this period coincides with the peak of the rainy season, posing a risk of nutrient leaching if heavy rainfall occurs shortly after top-dressing, especially in Plinthosols.

Authors: Iseki, K., Ikazaki, K. [JIRCAS],
Batieno, B.J. [INERA]

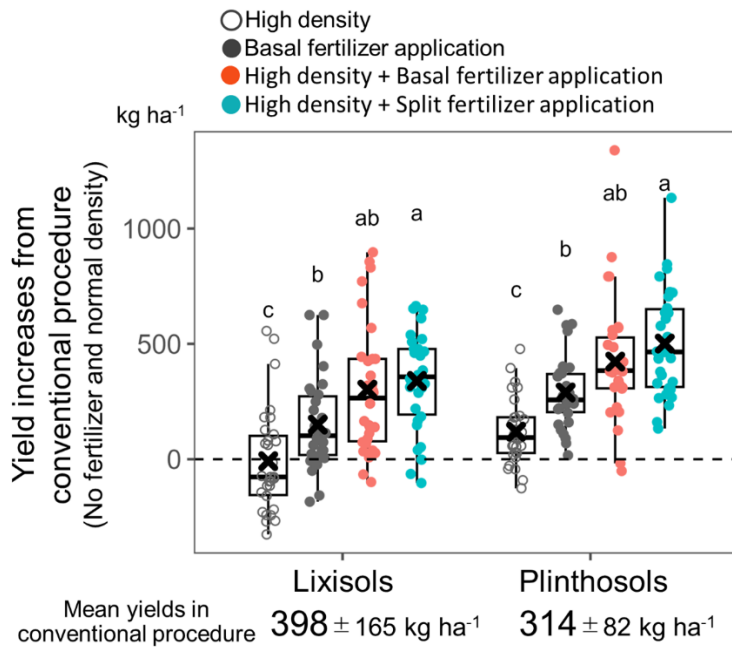


Fig. 1. Effects of fertilization and high plant density on cowpea yield in the dominant soil types of Sudan Savanna

Results of cultivating three cowpea varieties in the central region of Burkina Faso in 2018 and 2019. Each treatment shows variation over 2 years, with 3 varieties and 5 repetitions (n=30). Different letters indicate significant differences in means at P<0.05. The 'x' symbol represents the mean value.

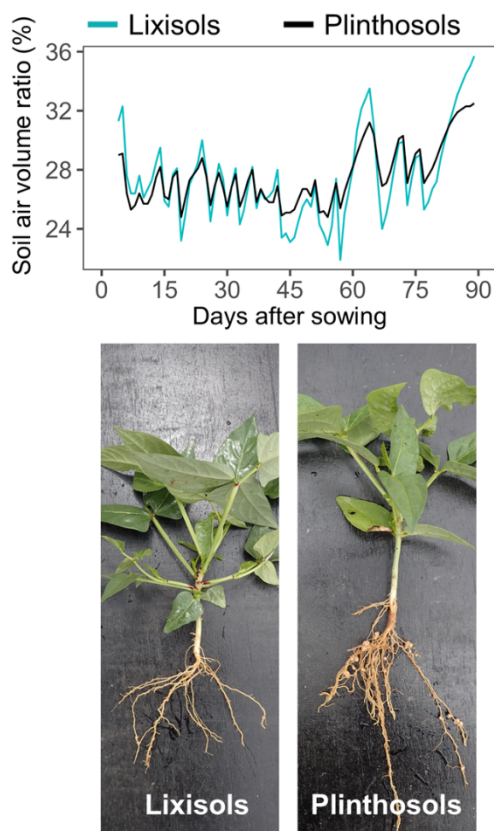


Fig. 2. Changes in soil air-volume ratio during the growth period (top) and appearance of cowpea root in each soil type (bottom)

Top: Lixisols are more prone to a decrease in soil air-volume ratio immediately after rainfall compared to Plinthosols, making them susceptible to waterlogging due to oxygen deficiency shortly after rainfall. Bottom: Cowpea grown in Lixisols showed minimal nodulation, and its root development was poorer compared to that in Plinthosols. The photos were taken in each soil type at four weeks after sowing.

Reference: Iseki et al. (2023) *Field Crops Research* 292: 108825. © The Author(s) 2023
<https://doi.org/10.1016/j.fcr.2023.108825>
 Figures reprinted/modified with permission.

Estimating the impact of climate change on cowpea production in Sudan Savanna using field cultivation data

In the semi-arid region of West Africa known as the Sudan Savanna, cowpea — a drought-resistant legume crop — is widely cultivated. Despite its importance as a protein source in the region, the yield per unit area is extremely low, and there are concerns about the increasing impact of extreme weather events such as heavy rainfall and drought due to climate change in the future. Addressing climate change, including predicting future production variability and identifying its causes, is urgently needed.

Yield prediction models can estimate crop yields by inputting meteorological conditions such as rainfall and temperature, as well as information about soil fertility and water characteristics. However, existing models targeting cowpea are specialized in predicting yields in optimal environments with minimal environmental stress, making it difficult for them to be applied to the harsh environments in Africa. To reveal the impact of climate change on cowpea production, this study aims to improve the accuracy of yield prediction models by utilizing field cultivation data in the Sudan Savanna accumulated in previous studies.

We created a yield prediction model using data from the cultivation of 20 cowpea varieties (n=1380) over four years with varying rainfall conditions in two representative soil types, Lixisols and Plinthosols, in the region. This allowed us to estimate yields in a wide range of environments, including dry and wet conditions (Fig. 1). Based on the latest global climate change predictions (Coupled Model Intercomparison Project Phase 6, CMIP6), it is forecasted that in West Africa, over the next 30 years, rainfall during the cowpea cultivation period (July to October) as well as the number of days with heavy rainfall exceeding 30 mm will increase (Fig. 2 top). The estimated yield model revealed that with increased rainfall and more days of heavy rainfall, cowpea yields in Lixisols will significantly decrease (Fig. 2 bottom). Furthermore, it is predicted that although cowpea yield reductions during drought periods will be mitigated compared to the present, drought-induced yield reductions will continue to be most severe in Plinthosols (Fig. 3).

Lixisols are relatively fertile and have high yields, making them significant areas for crop production. However, it is anticipated that excessive soil moisture stress will worsen due to increased rainfall, necessitating measures such as introducing tolerant varieties. In Plinthosols, drought-induced yield reductions are relatively greater than the reduction caused by excessive soil moisture, highlighting the need to control drought impact in the future.

Authors: Iseki, K., Ikazaki, K., Sakai, T. [JIRCAS], Iizumi, T. [NARO], Shiogama, H. [NIES], Imada, Y. [Tokyo Univ.], Batiemo, B.J. [INERA]



Lixisols
(1 month after sowing, 2016)



Plinthosols
(Harvesting time, 2017)

Fig. 1. Cultivation of cowpea in two dominant soil types in the Sudan Savanna

Twenty local varieties were cultivated for four years (2016-2019) in two dominant soil types in Sudan Savanna, namely Lixisols and Plinthosols. Lixisols (left) are prone to waterlogging shortly after rainfall, while Plinthosols (right) are susceptible to drought due to intermittent rainfall cessation.

Future changes in rainfalls during July-October

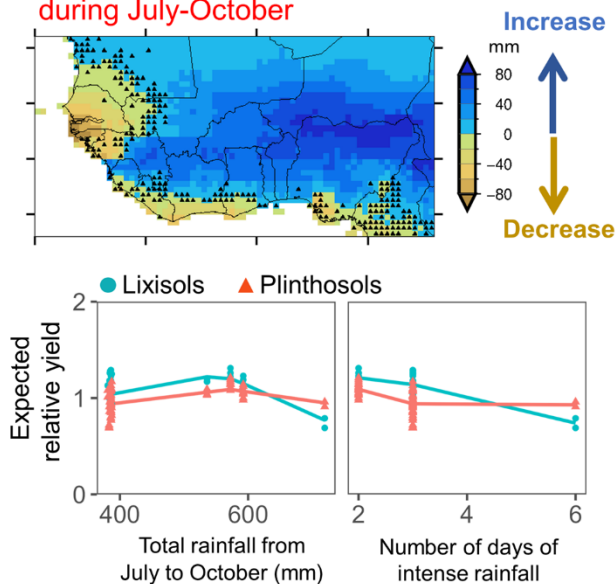
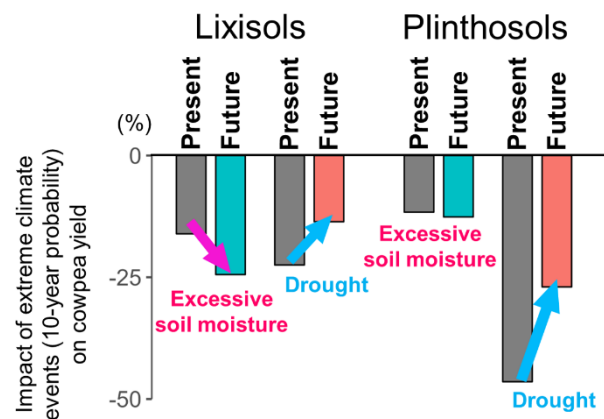


Fig. 2. Predictions of rainfall changes in West Africa and cowpea yield responses

(Top): Future predictions (2020-2049) compared to the present (1990-2019) regarding total rainfall during the cowpea growth period (mid-July to mid-October). Analysis results from CMIP6 simulations. Black dots indicate locations where the changes are statistically significant at the 5% level. (Bottom): Predicted relative yield in response to increased rainfall and number of heavy rainfall days (30 mm or more per day). The line represents local polynomial regression.



- Excessive soil moisture will have severe impact
- Drought impact will be reduced

Fig. 3. Impact of extreme weather events on cowpea yields in different soil types

Comparison of cowpea yield reduction rates in Lixisols and Plinthosols during excessive soil moisture stress and drought stress, comparing the present (1990-2019) and future (2020-2049).

Reference: lizumi et al. (2023) *Agricultural and Forest Meteorology* 344: 109783. © The Author(s) 2023
<https://doi.org/10.1016/j.agrformet.2023.109783>
 Figures reprinted/modified from lizumi et al. (2023).

Kinoshita and Shiranui, soybean varieties resistant to Asian soybean rust, have a second resistance gene

Asian soybean rust (ASR) is a major soybean disease that causes early yellowing and defoliation of soybean, resulting in reduced yield. This disease is widespread in soybean production areas around the world, especially in tropical and subtropical regions, and is a serious impediment to the stable supply of soybeans to international markets. In recent years, the susceptibility of the ASR pathogen to fungicides has decreased, resulting in increased control costs and environmental impact. Soybean varieties with resistance genes (*Rpp*) against ASR have since been developed in various regions. The soybean varieties Kinoshita and Shiranui were identified in 2008 as ASR-resistant varieties carrying *Rpp5*. These two varieties have shown resistance to many soybean rusts in various regions and are widely used in Latin America and Asia as parents for resistance variety development. However, their resistance to a wide range of rusts suggested that both varieties may also possess resistance other than *Rpp5*. Therefore, this study was conducted to determine the resistance potential of the Kinoshita and Shiranui varieties in order to appropriately and effectively utilize their resistance to a wide range of ASR pathogens in variety development.

The resistant varieties Kinoshita and Shiranui were crossed with susceptible varieties to produce F₂ populations. Each F₂ population was inoculated with the Japanese ASR strain E1-4-12 and the Brazilian strain BRS-2.5, which differ greatly in virulence, and evaluated for ASR resistance-related traits, respectively. QTL analysis of resistance-related traits was performed to identify resistance loci for each pathogen strain. QTL analysis revealed that Kinoshita and Shiranui possess loci *Rpp3* and *Rpp5*, which exhibit resistance to ASR strains E1-4-12 and BRP-2.5, respectively (Fig. 1). The *Rpp3* carried by both varieties was resistant only to strain E1-4-12 of the two strains used in this study, and the *Rpp5* of both varieties was effective only against strain BRP-2.5. The *Rpp5* and *Rpp3* of the Kinoshita and Shiranui varieties have similar genetic effects as well as genetic loci, suggesting that the two varieties may have the same or very similar resistance-type alleles in *Rpp5* and *Rpp3*, respectively (Table 1).

Because ASR pathogen in the soybean field is known to be diverse, both *Rpp5* and *Rpp3* should be introduced when Kinoshita and Shiranui are used for developing varieties with ASR resistance that have the same levels of resistance as Kinoshita and Shiranui. For the two resistance loci *Rpp3* and *Rpp5*, the use of DNA markers flanking and sandwiching the loci allows for effective and efficient selection for resistant plants in breeding for ASR resistance.

Authors: Yamanaka, N. [JIRCAS] and Aoyagi, L. N. [JIRCAS, Present address: NARO]

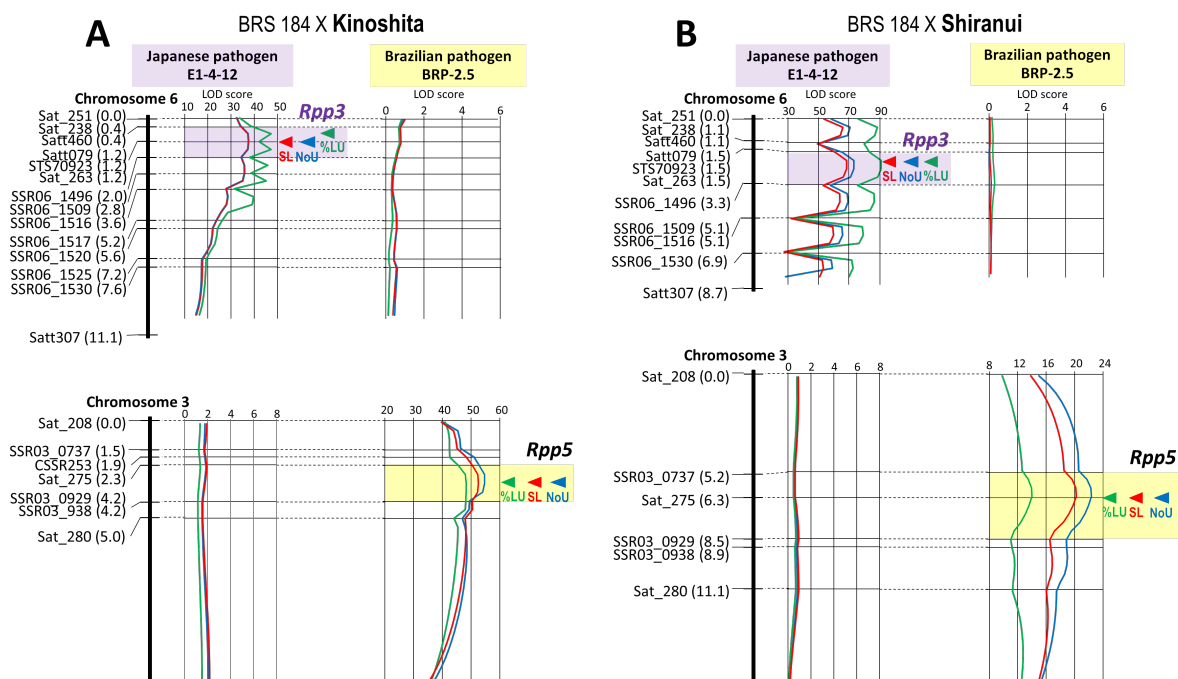


Fig. 1. Genetic maps around resistance loci *Rpp3* and *Rpp5* for Asian soybean rust in Kinoshita (A) and Shiranui (B) mapping populations

Each mapping population was created by crossing with the susceptible variety BRS 184. The DNA marker names and genetic distances from the top marker are shown on the left side of each linkage group, and the LOD values and their peak positions in QTL analysis for resistance-related traits (NoU: numbers of uredinia per lesion; %LU: frequency of lesions with uredinia; SL: Sporulation level) against E1-4-12 and BRP-2.5 strains are shown on the right side of each linkage group.

Table 1. Genetic effects and variance explained (VE) of the resistance genes *Rpp3* and *Rpp5* in the number of uredinia per lesion (NoU)

Parents of population	Resistance gene	Nearest marker	Pathogenic strain	Additive effect ¹⁾	Dominance effect ¹⁾	Variance-explained (%)
BRS 184 × Kinoshita	<i>Rpp5</i>	SSR03_0929	BRP-2.5	-1.15	-0.03	82.60%
	<i>Rpp3</i>	Sat_263	E1-4-12	-0.81	-0.74	51.50%
BRS 184 × Shiranui	<i>Rpp5</i>	Sat_275	BRP-2.5	-0.97	-0.09	52.29%
	<i>Rpp3</i>	Sat_263	E1-4-12	-0.82	-0.81	52.37%

¹⁾ Genetic effects (additive and dominant effects) are relative effects of the resistant (Kinoshita or Shiranui) allele to the susceptible (BRS 184) allele. *Rpp5* of Kinoshita and Shiranui are codominant due to their less dominant effects, while *Rpp3* of both varieties are completely dominant.

An integrated environmental control system and supplemental lighting increase strawberry production in subtropical regions

Strawberries (*Fragaria × ananassa* Duch.) are popular fruits consumed worldwide, and the demand for high-quality strawberries has been increasing in tropical and subtropical regions. This study aimed to elucidate the effects of environmental control and daytime LED supplemental lighting on strawberry production in a subtropical climate. Two strawberry cultivars, namely 'Yotsuboshi' and 'Benihoppe,' were grown by forcing culture in three greenhouses: (1) conventional greenhouse, with side vents open and no other environmental controls; (2) controlled environment (CE) greenhouse, equipped with an integrated environmental control system to cool air and growing medium; and (3) CE and LED greenhouse (CE&LED), equipped with an integrated environmental control system and LED supplemental lighting during the day.

Daily mean air and growing medium temperatures are lower in CE and CE&LED than in the conventional due to the combination of nighttime cooling, ventilation, shading, fogging, and medium cooling systems (Table 1). Even in the subtropical region, the temperature in greenhouses could be kept cooler by integrated environmental control. On Ishigaki Island, where the experiment was conducted, photosynthetic photon flux density (PPFD) increases in CE&LED in winter regardless of weather conditions (Fig. 1a, b). However, after April, when daily solar radiation exceeds 20 MJ m^{-2} , PPFD does not differ among greenhouses on sunny days (Fig. 1c). Conversely, even after April, PPFD increases with LED supplemental lighting during cloudy days (Fig. 1d). The integrated environmental control allows CE to produce yields comparable to the mean yield in Japan (Fig. 2). Environmental control also improves the percentage of marketable fruits weighing 6 g or more. Yield in CE&LED has significantly increased compared to CE. The number of fruits harvested and soluble solid content (SSC) in fruit increase when environmental control and LED supplemental lighting are used together (Table 2).

By introducing the integrated environmental control system, strawberry yield and quality improve in hot and humid environments such as subtropical regions. In addition, the combination of environmental control and supplemental daytime LED lighting is an effective technique for improving yield and fruit quality. On the other hand, since the effect is limited in environments where solar radiation exceeds 20 MJ m^{-2} , it is necessary to consider local weather conditions when introducing LED lighting.

Authors: Nakayama, M. [JIRCAS],
Nakazawa, Y. [CITIZEN ELECTRONICS Co., Ltd.]

Table 1. Daily mean air temperatures and mean growth medium temperatures by month

Greenhouse	Nov	Dec	Jan	Feb	Mar	Apr	May
<i>Daily mean air temperature</i>							
Conventional	23.1	21.5	20.0	19.3	23.1	25.5	25.3
CE	19.9	18.4	17.7	17.8	21.2	23.2	22.6
CE & LED	21.1	19.1	18.8	18.9	21.5	22.8	22.5
<i>Mean growth medium temperature</i>							
Conventional	23.2	21.8	21.2	19.9	23.9	26.8	26.5
CE	17.2	16.7	16.3	16.6	17.8	18.9	18.7
CE & LED	18.2	17.3	17.1	17.4	18.8	19.8	19.8

Air temperature was measured at a height of 1.5 m in the center of the greenhouse, and medium temperature was measured at a depth of 5 cm between plants.

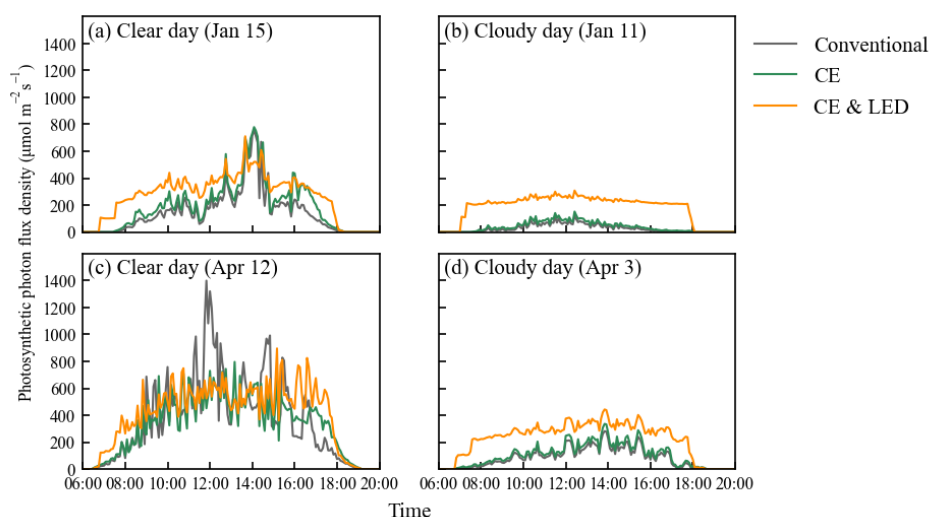


Fig. 1. Daily photosynthetic photon flux density in the conventional, controlled environment (CE), and LED (CE&LED) greenhouses on sunny and cloudy days

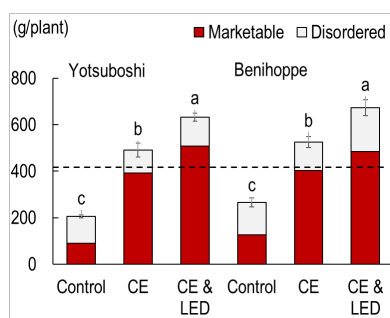


Fig. 2. Total and marketable yield Marketable fruits weighing 6 g or more. Different letters indicate significant differences at the 5% level. The dashed line indicates Japanese average (410 g/plant).

Table 2. Number of fruits, fruit weight, and soluble solid content (SSC)

	Number of fruits (fruits/plant)	Fruit weight (g)	SSC
<i>Greenhouse</i>			
Conventional	34.9 c	10.6 b	7.4 c
CE	45.3 b	13.6 a	7.7 b
CE & LED	56.2 a	14.1 a	8.0 a
<i>Cultivar</i>			
Yotsuboshi	47.3 NS	12.5 NS	7.7 NS
Benihoppe	43.7	14.5	7.7

Different letters indicate significant differences at the 5% level.

Reference: Nakayama and Nakazawa. (2023) *Scientia Horticultura* 321: 112349. © Elsevier B.V. 2023
 Figures and tables reprinted/modified from Nakayama and Nakazawa (2023) with permission.

Improvement of sugarcane root characteristics through intergeneric hybridization between sugarcane and *Erianthus*

In order to improve crop productivity and sustainable production under climate change, crops that are tolerant to drought stresses need to be developed. Improving root characteristics is an important breeding target to increase the productivity of crops grown under drought conditions. In sugarcane (*Saccharum* spp. hybrid), an important crop for global food and energy production, there is concern about increasing drought damage and a need to improve drought tolerance through root improvement. However, there have been few reports on root improvement in sugarcane, and the limitations of improvement using existing breeding materials have been pointed out. *Erianthus arundinaceus*, a genetic resource of a closely related genus of sugarcane, has large and deeply developed roots, making it highly adaptable to drought. Its roots also show high deposition of lignin, which is one of the major components of plant cell walls and is also associated with drought stress tolerance. Therefore, it has great potential to be a promising breeding material for improving the root characteristics of sugarcane. This study evaluated the root characteristics of an intergeneric F₁ hybrid of sugarcane and *E. arundinaceus* to assess the potential for introducing the root characteristics of *E. arundinaceus* into sugarcane through intergeneric hybridization.

Field experiments were carried out at the Japan International Research Center for Agricultural Sciences using the sugarcane cultivar NiF8, *E. arundinaceus* clones, and their intergeneric F₁ hybrid J08-12. We evaluated root distribution from 0 to 120 cm depth and fiber composition. J08-12 and *E. arundinaceus* clones had greater root dry weight per stool and smaller shoot-root ratios than NiF8. Regarding root distribution, J08-12 and *E. arundinaceus* clones had significantly greater root dry weights and root length densities than NiF8 in the deep soil layers. Root lignin contents were low in NiF8, high in *E. arundinaceus* clones, and intermediate in J08-12. These results indicate that intergeneric hybridization of sugarcane and *E. arundinaceus* could successfully introduce root characteristics of *E. arundinaceus*, such as deep root distribution and high lignin content, into sugarcane. Improving sugarcane root characteristics through intergeneric hybridization with *E. arundinaceus* will be a powerful strategy to improve drought tolerance and achieve sustainable sugarcane production in the future.

Authors: Terajima, Y., Sugimoto, A., Takagi, H., Ando, S. [JIRCAS],
Tippayawat, A. [Khon Kaen Field Crops Research Center],
Irei, S. [Okinawa Prefectural Agricultural Research Center],
Hayashi, H. [Univ. of Tsukuba]

Table 1. Agronomic traits and root characteristics of the intergeneric F₁ hybrid J08-12

Experiment	Clone	Dry matter yield (t ha ⁻¹)	Stalk number (stalks ha ⁻¹)	Root dry weight (g stool ⁻¹)	Shoot-root ratio	Lignin content (mg g ⁻¹ -DW)
Exp. 1	J08-12	31.9 ns ^b	131,305 *	80 ns	18 *	163 ns
	NiF8	20.3	63,161	24	35	140
	IJ76-349	58.8 *	117,041 *	251 *	10 *	193 *
	JW630	46.1 *	552,315 *	170 *	12 *	228 *
Exp. 2	J08-12	31.6 ns	145,688 ns	65 ns	26 ns	166 *
	NiF8	27.3	100,714	42	30	133
	JIRCAS1	51.7 *	588,810 *	214 *	16 *	199 *

* and n.s. indicate significant differences at $P < 0.05$ and no significant difference from NiF8, respectively, according to the Dunnett test. Exp. 1 is the mean of three years of data harvested in January 2011, January 2012, and December 2012. Exp. 2 is the mean of two years of data harvested in January 2014 and February 2015. NiF8 is the sugarcane cultivar. IJ76-349, JW630, and JIRCAS1 are *Erianthus* clones. J08-12 is an intergeneric F₁ hybrid between NiF8 and JIRCAS1.

Table 2. Root length density of J08-12 at different soil depths (cm cm⁻³)

Experiment	Clone	Soil depth					
		0-20 cm	20-40 cm	40-60 cm	60-80 cm	80-100 cm	100-120 cm
Exp. 1	J08-12	1.07 ns ^b	0.49 ns	0.41 *	0.30 ns	0.23 ns	0.24 *
	NiF8	0.85	0.61	0.20	0.11	0.08	0.04
	IJ76-349	3.18 *	1.20 *	0.66 *	0.30 ns	0.34 *	0.37 *
	JW630	3.03 *	1.31 *	0.62 *	0.33 ns	0.31 *	0.26 *
Exp. 2	J08-12	1.55 ns	0.61 ns	0.53 ns	0.45 *	0.29 *	0.21 *
	NiF8	1.28	0.55	0.36	0.18	0.09	0.04
	JIRCAS1	2.53 ns	1.09 ns	0.65 ns	0.56 *	0.32 *	0.32 *

* and n.s. indicate significant differences at $P > 0.05$ and no significant difference from NiF8, respectively, according to the Dunnett test. Exp. 1 evaluated the root of the second ratoon crops, which was harvested in January 2011, January 2012, and December 2012. Exp. 2 evaluated the root of the first ratoon crop, harvested in January 2014 and February 2015.

**Fig. 1. Amount (top) and distribution (bottom) of roots of J08-12**

J08-12 has more roots and deeper root distribution than NiF8 (Exp. 1).

Reference: Terajima et al. (2023) *Field Crops Research* 297: 108920. © The Author(s) 2023
The tables and figure were reprinted/modified from Terajima et al. (2023).

Photosynthetic capacity of passion fruit genotypes at high temperatures is determined by transpiration capacity under non-stressed conditions

Passion fruit (*Passiflora* spp.) is mostly indigenous to the tropical highlands, generally with decreasing growth and productivity in high temperature conditions. Purple passion fruit (*P. edulis*) has lower juice acidity with excellent fresh eating quality, but its growth and productivity are severely inferior at high temperatures. Yellow passion fruit (*P. edulis* f. *flavicarpa*) is tolerant to high temperatures and can be cultivated in some tropical lowlands, but its juice shows high acidity and is not suitable for fresh consumption. Hybrids of these species have been bred in various areas of the world. However, summer productivity remains poor, and little is known about the leaf photosynthetic responses to high temperatures, which can affect growth during hot summers.

We measured the individual leaf photosynthesis of 13 genotypes of passion fruit at high temperatures above 30°C using a portable gas-exchange system in a growth chamber under precisely controlled environments (Fig. 1) to analyze the traits that correlated highly with photosynthetic capacity. At leaf temperatures up to 40°C, gross and net photosynthetic rates decreased mainly due to stomatal closure, while above 40°C, only the net photosynthetic rate decreased due to increased respiration (Fig. 2). The reduction in photosynthesis at high leaf temperatures above 35°C was strongly correlated ($p < 0.01$) with transpiration rate and stomatal conductance under non-stress conditions (leaf temperature of 30°C), and genotypes with well-opened stomata exhibiting higher transpiration rates showed a smaller net photosynthetic rate reduction at high temperatures (Fig. 3). The reductions in net photosynthetic rate at high temperatures and the values of transpiration rate and stomatal conductance under non-stress conditions (leaf temperature of 30°C) were strongly correlated with stomatal size ($p < 0.01$) in 9 genotypes of *P. edulis* group (Table 1), excluding 4 genotypes of lowland relatives (*P. alata* and *P. laurifolia*). These results indicate that genotypes with larger stomatal sizes maintained higher net photosynthetic rates at extremely high leaf temperatures above 40°C and had higher net photosynthetic rates and stomatal conductance under non-stress conditions.

This information can be useful for further selection of passion fruit genotypes with resilience to ongoing global warming. We need to consider separately the application to crossbreeding using lowland relatives, in which stomatal traits did not clearly correlate with transpiration capacity; however, transpiration capacity under non-stress conditions can be one of the target traits for breeding passion fruit genotypes that are highly tolerant to high temperatures.

Authors: Matsuda, H., Takaragawa, H. [JIRCAS]



Fig. 1. Measurement in a growth chamber

Photosynthesis measurements were conducted in 13 passion fruit genotypes.

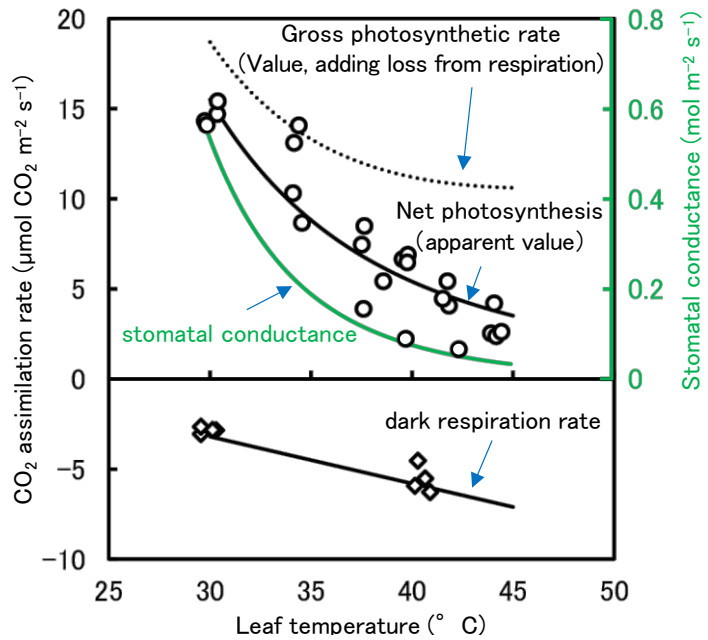


Fig. 2. Relationship between leaf temperature and photosynthetic rate, respiration rate, and stomatal conductance (cultivar 'Ruby Star')

Sigmoidal curve and linear regression were performed.

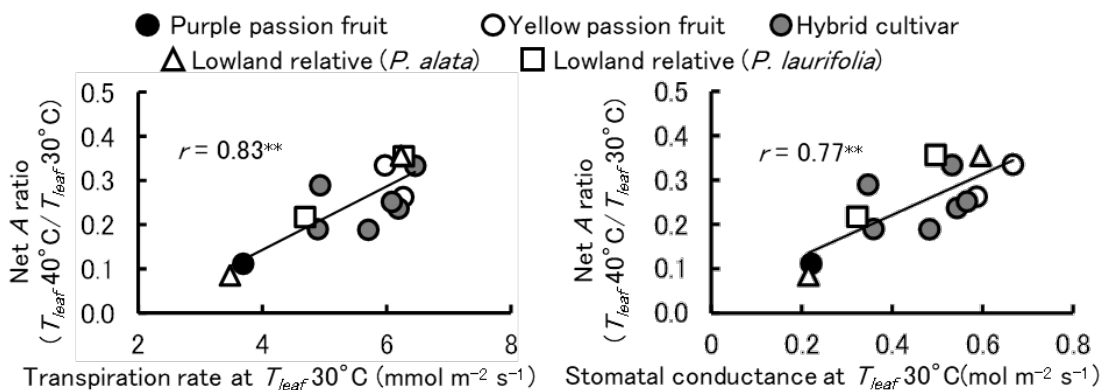


Fig. 3. Relationship between photosynthetic rate (A) reduction at high temperature and transpiration under non-stress condition at leaf temperature (T_{leaf}) of 30°C

** represents significant correlation at $p < 0.01$.

Table 1. Correlation coefficients between photosynthetic reduction and transpiration capacity and stomatal traits (excluding lowland relatives)

	Stomatal density	Stomatal size
Net A ratio ($T_{leaf} 35^{\circ}\text{C}/T_{leaf} 30^{\circ}\text{C}$)	- 0.76 **	0.43 NS
Net A ratio ($T_{leaf} 40^{\circ}\text{C}/T_{leaf} 30^{\circ}\text{C}$)	- 0.55 NS	0.90 **
Net A ratio ($T_{leaf} 45^{\circ}\text{C}/T_{leaf} 30^{\circ}\text{C}$)	- 0.60 NS	0.82 **
Transpiration rate at $T_{leaf} 30^{\circ}\text{C}$	- 0.67 *	0.79 **
Stomatal conductance at $T_{leaf} 30^{\circ}\text{C}$	- 0.59 NS	0.88 **

* and ** indicate significant correlation at $p < 0.05$ and $p < 0.01$, respectively. NS means no significance.

Reference: Matsuda and Takaragawa (2023) *The Horticulture Journal* 92: 412–423.

© The Japanese Society for Horticultural Science

The figures were reprinted/modified from Matsuda and Takaragawa (2023) with permission.

**Japan International Research
Center for Agricultural Sciences**

Headquarters (Tsukuba)

1-1 Ohwashi, Tsukuba, Ibaraki
305-8686, JAPAN
TEL : +81-29-838-6313
FAX : +81-29-838-6316

**Tropical Agriculture Research Front
(TARF)**

1091-1 Maezato-Kawarabaru, Ishigaki
Okinawa, 907-0002, JAPAN
TEL : +81-980-82-2306
FAX : +81-980-82-0614

<https://www.jircas.go.jp/>

